MAX-PLANCK-INSTITUT FÜR PLASMAPHYSIK

GARCHING BEI MÜNCHEN

# Quasilinear Ion Distribution Function During First Harmonic Ion Cyclotron Heating

Marco Brambilla

IPP 5/56 December 1993

*Die nachstehende Arbeit wurde im Rahmen des Vertrages zwischen dem Max-Planck-Institut für Plasmaphysik und der Europäischen Atomgemeinschaft über die Zusammenarbeit auf dem Gebiete der Plasmaphysik durchgeführt.*

# QUASILINEAR ION DISTRIBUTION FUNCTION DURING FIRST HARMONIC ION CYCLOTRON HEATING

**Marco Brambilla**

**Max–Planck Institut für Plasmaphysik**
**Euratom Association**
**Garching bei München, Germany.**

ABSTRACT

The quasilinear modification of the ion distribution function during first harmonic ion cyclotron (FHIC) heating is investigated both with a simple already well established analytic one–dimensional approach, and with a new two dimensional steady state solver of the quasilinear kinetic equation, SSFPQL. By accepting to disregard the effects of ion trapping in banana orbits, but including finite Larmor radius effects, the latter code has been made much faster than full surface–averaged codes; yet it can provide most of the relevant information on the suprathermal ion tail produced by this heating method. With SSFPQL we confirm that the one–dimensional model gives fair approximations for global properties of the distribution function, such as the average energy content of the tail and the fusion reactivity. On the other hand the tail is found to be very anisotropic, the increase of the parallel effective temperature being a small fraction of the total energy increase. Information on the anisotropy is essential to study the feedback of the fast ion tail on wave propagation and absorption, which is quite sensitive to the distribution of parallel velocities. The insight gained in the derivation and discussion of this model can be used to build a selfconsistent description of this heating scenario, whose implementation requires only a reasonable numerical effort.

Estimates of the effects of the suprathermal ion tail produced by first harmonic ion cyclotron heating on the heating rate and on the fusion reactivity are presented. In ITER, the suprathermal tritium population might lower the ignition temperature by a few keV, thereby reducing the h.f. power requirements. It is also pointed out that the conditions for FHIC heating in ASDEX Upgrade at intermediate density and power are sufficiently similar to those of ITER to make such an experiment particularly interesting.

## 1 – Introduction.

Ion cyclotron heating at the first harmonic $\omega = 2\Omega_{ci}$ (FHIC heating) is presently regarded as the most likely option for auxiliary h.f. heating in ITER and in the tokamak reactor. Being a finite Larmor radius effect, the efficiency of FHIC heating increases with increasing plasma pressure; for ITER parameters it should be competitive with that of minority heating, while dispensing with the introduction of minority ions which would dilute the reacting species, and whose concentration could be difficult to control. In ITER, moreover, the production of a population of suprathermal ions by FHIC heating will enhance the reactivity, and can be exploited to relax the requirements on heating and confinement to reach ignition. On the other hand, FHIC heating is be relatively inefficient in low temperaturature ohmic plasmas: a sufficient power must be available to overcome the initial unfavorable phase. Once a suprathermal ion tail begins to develop, however, the efficiency should rapidly improve.

To model FHIC heating selfconsistently, understanding of the propagation and absorption of the Fast Wave in the plasma must be combined with the evaluation of the ion distribution function under the effects of heating. The first topic has been reviewed in [1]. The present report is devoted to the solution of the quasilinear kinetic equation which governs the long–term evolution of the distribution function of the heated ions,

$$\frac{dF_i}{dt} = \left(\frac{\partial F_i}{\partial t}\right)_{QL} + \left(\frac{\partial F_i}{\partial t}\right)_{coll} + \left(\frac{\partial F_i}{\partial t}\right)_{loss} \tag{1}$$

where the first term describes the quasilinear diffusion due to resonant wave particle interactions, the second term is the Fokker-Planck collision operator, and the last term describes losses, e.g. due to radial transport. In this report we will briefly discuss reasonable approximations for the first two operators; losses, however, will be not considered.

In principle, the evaluation of the quasilinear diffusion operator in the r.h. side of Eq. (1) requires the knowledge of both amplitude and polarization of the h.f. electric field in the absorption region, which in turn depend on the ion distribution function. Selfconsistent modelling therefore appears to demand a close coupling between a wave code and a Fokker–Planck code. The wave code must take into account the whole spectrum radiated by the antenna and the complicated toroidal geometry, while the Fokker–Planck code must solve the kinetic equation on a sufficient number of magnetic surfaces. Consistency can be realized only by iterating between the two codes until convergence is reached. This procedure is extremely heavy, and to our knowledge it has never been fully implemented.

The situation can be substantially improved, however, by developing appropriate approximations. In section 2 we will show that in the case of IC heating the information required from the wave code for the construction of the quasilinear operator essentially reduces to the knowledge of the power deposition profile. In [2], on the other hand, taking advantage of the fact that the wavelength of the Fast Wave is always much larger than the thermal ion Larmor radius, we have shown that the wave code in turn needs only the first few "reduced" distributions of the parallel velocity, obtained by integrating the ion distribution function over the perpendicular velocity after multiplication with a low power of $v_\perp$. A model distribution function which accurately reproduces the results of numerical integration of Eq. (1) and greatly facilitates the evaluation of the reduced distributions is one of the results of the present work. Combining these results, a much looser and easily implemented coupling between the two codes becomes sufficient to obtain accurate self–consistent results.

Since our considerations are for the most part analytic, we will not discuss here surface averaging of the collisional operator in tokamak geometry [3]. On the other hand, to justify our approximations, in the next section we will rederive in some length the quasilinear operator. In particular, using properties of the dispersion relation of the Compressional Wave in the ion cyclotron frequency range, we will justify explicitly a few approximations which considerably simplify the form of the quasilinear diffusion coefficient, and which are usually taken for granted in the literature. We will also show that a full agreement of the energy balance obtained from a wave code and from the Fokker–Planck code is unachievable in practice, particularly because different approximations with respect to finite Larmor radius effects are unavoidable (and justified) in the two codes. Instead, the energy balance equation should be used to renormalize the absolute value of the quasilinear diffusion coefficient in the Fokker–Planck code. These considerations show that the "brute force" coupling of the two codes not only is very difficult to implement, but the kind of consistency it offers is largely illusory. They suggest instead a much looser coupling between the wave propagation and the kinetic aspects of the problem, based on semi–analytic considerations such as those developed in this report.

In section 3 we present analytic solutions of a reduced, one–dimensional kinetic equation obtained neglecting the anisotropy of IC heating, along the lines of the well–known Stix solution for the minority distribution functions [4]. Similar analytic solutions have been widely used in the literature [5]–[7]. In the case of first harmonic heating the analytic approach is justified by the fact that deviations from a thermal distribution are not very large, because essentially all ions (or at least half of them in a D–T plasma) are affected by the heating, so that the power available per ion is relatively small.

Nevertheless with appropriate modifications most of our conclusions can be extended also to the case of minority heating, where the power per ion can be substantially larger.

The elementary one–dimensional theory makes accurate predictions for global properties of the distribution function, such as the effective temperature of the suprathermal ion population, the quasilinear increase of IC absorption, and the reactivity enhancement in thermonuclear plasmas. Nevertheless it is not fully adequate to investigate the effects of distortion of the distribution function on wave propagation and absorption, which are specially sensitive to the distribution of parallel velocities. For this purpose, therefore, some information on the anisotropy of the distribution function is also required [2]. To obtain this information, we have written a new two–dimensional steady–state quasilinear Fokker–Planck solver SSFPQL. This code, which will be described in details elsewhere, has been developed building on the insight gained from the analytic work of section 3. It does not take into account trapping of ions in banana orbits, hence it cannot be used to follow ions to very large energies. On the other hand it includes fully finite Larmor radius effects in the quasilinear operator, and, with a modest numerical effort, can provide the information required to investigate wave propagation and absorption, enhanced fusion reactivity, the effects of suprathermal ions on MHD equilibrium and stability, and so on. Moreover, it is extremely fast. It could for example be coupled with a ray–tracing wave code in order to determine the ion distribution function on a large number of magnetic surfaces, without substantially increasing the computation time.

After a brief presentation of SSFPQL, results of its application to first harmonic heating in ASDEX Upgrade and ITER are presented in section 4. They confirm that the estimates of the total energy and of the effective temperature of the suprathermal tail obtained from the one–dimensional approximation are quite good, in spite of the fact that the suprathermal ion distribution is very anisotropic. This is because, as anticipated, the tail begins at relatively large energies, hence contains relatively few ions, which however are only weakly collisional. The anisotropy is so strong that the distribution of parallel velocities $F_i(v, \mu = 0)$ is barely distinguishable from an unperturbed Maxwellian. This suggests a simple yet accurate analytic representation of the total distribution function which can be used to evaluate analytically the dielectric tensor elements and the coefficients of the wave equation. In this way quasilinear effects on wave propagation and absorption can be taken into account reliably with a minimum numerical effort.

A few conclusions are presented in section 5. It is interesting in particular that as far as the ion distribution function is concerned, a situation comparable to the one

prevailing in ITER can be obtained in ASDEX Upgrade already at moderate total IC power. We will also show that in spite of its moderate energy content the suprathermal tail is sufficient to enhance appreciably power absorption from the waves, and also, in the ITER case, the fusion reactivity. Although the latter effect will only modestly improve the $Q$ of the ignited plasma, it can be useful in that it can significantly reduce the power requirements to reach ignition.

## 2 – The quasilinear kinetic equation for first harmonic heating.

*2.1 – The linearized Fokker–Planck operator.* For our purposes it is sufficient to regard the heated ions as test particles colliding with a thermal background plasma. Due to the weak non–linearity of the Fokker–Planck operator this is mostly an acceptable approximation. In the case of FHIC heating, a further justification is that due to the low power per particle one does not expect really large deviations from thermal equilibrium.

The linearised collision operator for the heated species can be written

$$\left.\frac{\partial F_i}{\partial t}\right)_{coll} = \sum_\beta \nu^{i/\beta}\left\{\frac{1}{v^2}\frac{\partial}{\partial v}v^2\left[\Psi(\gamma_{i\beta}v)\left(\frac{1}{2v}\frac{\partial f^i}{\partial v}+\frac{T_i}{T_\beta}f^i\right)\right]\right.$$
$$\left.+\frac{\Theta(\gamma_{i\beta}v)}{2v^3}\frac{\partial}{\partial\mu}\left((1-\mu^2)\frac{\partial f^i}{\partial\mu}\right)\right\} \tag{2}$$

where the sum extends over electrons and background ions. The second term describes pitch–angle scattering. Velocities are normalised to an appropriate thermal velocity $v_{th\beta} = (2T_\beta/m_\beta)^{1/2}$ (for the heated species, $T_i$ can be chosen to be the temperature $T_o$ before heating), and $\gamma_{i\beta} = v_{thi}/v_{th\beta}$. Moreover, with $u_\beta = \gamma_{i\beta}v$,

$$\Psi(u_\beta) = \frac{\Phi(u_\beta)}{u_\beta^2}$$
$$\Theta(u_\beta) = \frac{1}{2u_\beta}\frac{d\Phi}{du_\beta}+\left(u_\beta^2-\frac{1}{2}\right)\frac{\Phi(u_\beta)}{u_\beta^2} \tag{3}$$

with

$$\Phi(u_\beta) = \frac{4}{\sqrt{\pi}}\int_0^{u_\beta} u^2\,e^{-u^2}\,du = -\frac{2}{\sqrt{\pi}}u_\beta\,e^{-u_\beta^2}+\mathrm{Erf}\,(u_\beta) \tag{4}$$

The linearized FP operator conserves particles, but energy is lost to the thermal bath constituted by the background plasma. This corresponds well to the real situation, and greatly simplifies coupling of a linearized FP solver to a tokamak transport code, if required.

We recall that the coefficients of the linearized collisional operator can be further simplified following the well–known procedure due to Stix [4]. In the electron contribution it is sufficient to retain the leading term of the small argument expansion of $\Psi(u_e)$,

$$\Psi(u_e) \simeq k_o \frac{v_{thi}}{v_{the}} v \tag{5}$$

while $\Theta(u_e)$ can be neglected altogether. For the ion–ion collision terms Stix suggests the approximations

$$\begin{aligned} \Psi(u_\beta) &\simeq \frac{k_o u_\beta}{1 + k_o u_\beta^3} \\ \Theta(u_\beta) &\simeq \frac{3k_o}{2} u_\beta^2 \, e^{-u_\beta^2} + \left(u_\beta^2 - \frac{1}{2}\right) \frac{k_o u_\beta}{1 + k_o u_\beta^3} \end{aligned} \tag{6}$$

where $k_o = 4/3\sqrt{\pi}$. The exact and approximate coefficients are compared in fig. 1: the error does not exceed a few percent.

*2.2 – The quasilinear diffusion operator for first harmonic heating.* We sketch here the derivation of the quasilinear diffusion operator, taking into account for simplicity only the contribution from the main resonance of $E_+$ at $\omega = 2\Omega_{ci}$. In this limit the quasilinear (QL) operator has the form

$$\left(\frac{\partial F_i}{\partial t}\right)_{QL} = \frac{1}{v_\perp} \frac{\partial}{\partial v_\perp} \left( v_\perp \, D_2(k_\perp, v_\perp) \frac{\partial F_o}{\partial v_\perp} \right) \tag{7}$$

Several approaches are available to obtain $D_2(k_\perp, v_\perp)$ in tokamak geometry. The simplest is to start from the diffusion coefficient derived by Kennel and Engelmann [8] for the homogeneous infinite plasma,

$$D_2^{KE}(k_\perp, v_\perp) = \frac{\pi}{4\omega} \left(\frac{Ze}{m}\right)^2 \sum_{\vec{k}} |E_+(\vec{k})|^2 \, J_1^2 \left(\frac{k_\perp v_\perp}{\Omega}\right) \delta\left(\frac{\omega - 2\Omega_c - k_\parallel v_\parallel}{\omega}\right) \tag{8}$$

and to average this expression over a magnetic surface. If for this purpose we assume $\Omega \simeq \Omega(0)\,(1 - (r/R)\cos\vartheta)$, we find

$$D_2(k_\perp, v_\perp) = \left\langle D_2^{KE}(k_\perp, v_\perp) \right\rangle = \frac{R}{8\Omega_o r |\sin\vartheta_o|} \left(\frac{Ze}{m}\right)^2 \sum_{\vec{k}} |E_+(\vec{k})|^2 \, J_1^2 \left(\frac{k_\perp v_\perp}{\Omega}\right) \tag{9}$$

where $\vartheta_o$ denotes the position where the resonance $2\Omega_o = \omega$ cuts the magnetic surface (a factor 2 takes into account that each magnetic surface crosses the resonance twice).

This procedure is not fully satisfactory, however, since it assumes implicitly that the h.f. field is a superposition of plane waves. This assumption is actually nearly correct, but is difficult to justify. It is therefore preferable to regard each transit through resonance as causing a small "random" change $\Delta v_\perp$, and to evaluate $D_2$ through its definition as a diffusion coefficient. Accordingly, $D_2$ is related to the average heating rate of the single particle:

$$D_2 = \left\langle \frac{\Delta v_\perp^2}{\Delta t} \right\rangle \simeq \frac{2}{m} \frac{dK_\perp}{dt} \tag{10}$$

This expression can be estimated directly in toroidal geometry. For this purpose, we can assume the validity of an Eikonal representation of the h.f. electric field,

$$\vec{E}(\vec{r},t) = \sum_{m_\vartheta, n_\varphi} \vec{E}(r;\, m_\vartheta, n_\varphi)\, e^{i(S(r;m_\vartheta,n_\varphi)+m_\vartheta\vartheta+n_\varphi\varphi-\omega t)} \tag{11}$$

with slowly varying amplitudes and rapidly varying phase. For each partial wave the local wavevector is defined by

$$\begin{aligned} k_r(m_\vartheta, n_\varphi, r, \vartheta) &= \partial S/\partial r \\ k_\eta(m_\vartheta, n_\varphi, r, \vartheta) &= \frac{m_\vartheta}{r}\cos\Theta - \frac{n_\varphi}{R}\sin\Theta \\ k_\perp^2 &= k_r^2 + k_\eta^2 \\ k_\parallel(m_\vartheta, n_\varphi, r, \vartheta) &= \frac{m_\vartheta}{r}\sin\Theta + \frac{n_\varphi}{R}\cos\Theta \end{aligned} \tag{12}$$

and must satisfy the dispersion relation of the fast wave. Admittedly, the Eikonal representation of the field fails in the vicinity of the mode conversion layer which accompanies the first harmonic cyclotron resonance. However, as discussed in [1], either this layer is outside the cyclotron absorption region (mode conversion regime), or it is washed away by Doppler–broadening (cyclotron damping regime). In both cases the Eikonal representation is adequate to investigate wave–particle cyclotron interactions (to the lowest significant order in the Larmor radius, moreover, the results obtained using the form (11) for the electric field could be easily generalised to the case in which this representation fails in the resonance region: it would be sufficient for this purpose to replace $k_\perp^2|E_+|^2$ by $|\vec{\nabla}_\perp E_+|^2$).

For a single transit through resonance we can evaluate $\Delta v_\perp$ by integrating the equation of motions iteratively, with the electric field taken along the unperturbed trajectory. This gives

$$\begin{aligned} v_+(t_o+T_b) \simeq\, & v_+(t_o)\, e^{-i\int_{t_o}^{t_o+T_b}\Omega d\tau} + \\ & \frac{Ze}{m}\,\mathrm{Re}\left\{ \sum_{m_\vartheta, n_\varphi} \int_{t_o}^{t_o+T_b} E_+(r';m_\vartheta,n_\varphi)\, e^{-i\left(h(t')-h_{eq}\right)} dt' \right\} \end{aligned} \tag{13}$$

Here $h(t')$ is the phase between the gyration velocity of the ion and the left-hand circular component of the electric field,

$$h(t') - h_{eq} = \int_{t_a}^{t'} \left(\omega - \Omega_c - k_\parallel v_\parallel\right) d\tau + \frac{k_\perp v_\perp}{\Omega_c} \sin\left(\phi_v - \psi_{\vec{k}} - \int_{t_o}^{t'} \Omega_c d\tau\right) \tag{14}$$

where $\tan\psi_{\vec{k}} = k_\eta/k_r$, and $h_{eq}$ is the value of $h$ value at the time $t_o$ when the particle crosses the outer equatorial plane. Developing the exponential in a series of Bessel functions, and averaging over all possible values of this phase, it is not difficult to obtain

$$\left\langle \frac{dK_\perp}{dt} \right\rangle \simeq \frac{Z^2 e^2}{8mT_b} \sum_{n_\varphi} \left| \mathrm{Re} \sum_{m_\vartheta} E_+(r; m_\vartheta, n_\varphi) \right. \\ \left. \sum_n J_{n-1}\left(\frac{k_\perp v_\perp}{\Omega}\right) \int_{t_o}^{t_o+T_b} e^{-ih_n(t')} dt' \right|^2 \tag{15}$$

where $T_b$ is the transit time between resonances, and

$$h_n(t') = \int_{t_o}^{t'} \left(\omega - k_\parallel v_\parallel - n\Omega_c\right) d\tau \tag{16}$$

We can assume that only the harmonic $n = 2$ satisfies the resonance condition

$$\frac{dh_n}{dt} = \omega - n\Omega_c - k_\parallel v_\parallel = 0 \tag{17}$$

within the tokamak cross–section. Excluding for simplicity the case of trapped particles with turning point close to the resonance, we then have

$$\int_{t_o}^{t_o+T_b} e^{-ih(t')} dt' \simeq \left(\frac{\pi}{|h''_{Res}|}\right)^{1/2} e^{-i\left(\frac{\pi}{4} + h_{Res}\right)} \tag{18}$$

From the average equations of motion we get

$$\frac{d^2h}{dt^2} = -\frac{d}{dt}\left(2\Omega_c + k_\parallel v_\parallel\right) \simeq -\frac{v_\parallel \sin\Theta}{r} \frac{\partial}{\partial\vartheta}\left(2\Omega_c + k_\parallel v_\parallel\right) \tag{19}$$

where $\tan\Theta = B_{pol}/B_{tor}$. For well passing particles on the other hand

$$\Delta t = T_b \simeq \frac{\pi r}{v_{\parallel eq} \sin\Theta} \tag{20}$$

Inserting these results into Eq. (10) and multiplying by 2 to take into account that there are two resonances on each magnetic surface, to lowest order in the inverse aspect ratio we finally find

$$D_2 = \frac{2}{m}\left\langle \frac{dK_\perp}{dt} \right\rangle \simeq \left(\frac{Z^2 e^2}{8m^2\Omega_o}\right)\left(\frac{R}{r|\sin\vartheta_{Res}|}\right) \\ \sum_{n_\varphi} \left| \mathrm{Re} \sum_{m_\vartheta} E_+(r, m_\vartheta, n_\varphi)\, J_1\left(\frac{k_\perp v_\perp}{\Omega}\right) e^{-i\left(\frac{\pi}{4} + h_{Res}\right)} \right|^2 \tag{21}$$

This result is essentially equivalent to Eq. (9); it specifies however more explicitly how the wave electric field at resonance enters the definition of $D_2$. Before proceeding, it is useful to make the following comments.

1) Averaging over $h_{eq}$ is justified if the particle gyrophases at two successive transits through resonance are uncorrelated. Both collisions [9] and deterministic stochasticity [10]–[11] due to the resonant wave–particle interactions efficiently contribute to phase decorrelation. Hence *a random–phase assumption for the field is not required for the validity of the quasilinear approximation.*

2) Contributions from partial waves with different toroidal wave numbers $n_\varphi$ are additive in an axisymmetric plasma. Contributions from partial waves with different poloidal wave numbers $m_\vartheta$, on the other hand, are subject to interference. Nevertheless a detailed knowledge of the phase relations is usually not required, since one of the following approximations can be made:

a) If $m_\vartheta v_\parallel \sin\Theta/r << n_\varphi v_\parallel \cos\Theta/R$ or $m_\vartheta v_\parallel \sin\Theta/r << \langle\omega - \Omega_c\rangle$ over most of the unperturbed trajectory, ('long' poloidal wavelengths) $h_{Res}$ does not depend appreciably on $m_\vartheta$; then the sum over $m_\vartheta$ gives just the total field $|E_+|^2$ of the partial wave $n_\varphi$ at resonance.

b) In the opposite limit ('short' poloidal wavelengths) averaging over the phases $h_{Res}$ reduces the last sum to a sum of separate contributions from each $m_\vartheta$.

Generally the first situation prevails in first harmonic heating.

3) The divergence of the expression (21) for $D_2$ when the magnetic surface is tangent to the resonance is due to the inadequacy of our simplified approach to deal with the confluence of two separate resonances. The correct surface averaging [12]–[13] must take into account trapped ions having turning points near resonance, and gives a large but finite result as $r\sin\vartheta_o \to 0$. For trapped particles (excluding those nwhich are 'barely' trapped) one has

$$T_o \simeq \frac{\pi r}{v_{\parallel eq}\lambda_{eq}^{1/2}\sin\Theta} \qquad \lambda_{eq} = \frac{r}{R_{eq}}\frac{v_{\perp eq}^2}{v_{\parallel eq}^2} > 1 \tag{22}$$

Hence the heating rate for such particles is a factor $2\lambda_{eq}^{1/2}$ larger than for passing particles. On the other hand, trapped particles 'see' the resonance only as long as their turning point $\vartheta_{tp} \simeq \lambda_{eq}^{-1/2}$ is larger than $\vartheta_{res}$ (i.e. occurs on the high–field side of the resonance). For our present purposes, however, we will neglect the resulting pitch angle dependence of $D_2$.

In the absence of losses, the two effects just mentioned result in the accumulation of high energy ions on large banana orbits with reflection point just to the outside of resonance. For ions reaching such orbits the surface averaging procedure used to derive Eqs. (21) is hardly justified, however, since they make large excursions from the average magnetic surface [14]. On the other hand, the number of such ions is likely to be relatively small, so that their production and radial diffusion can best be investigated with Montecarlo methods based on a test–particle approximation [15]. For the purposes of coupling the solution of the kinetic equation with wave codes it is plausible to assume that their presence can be neglected.

4) $D_2$ is proportional to the amplitude of the $E_+$ component of the electric field at $\vartheta = \vartheta_{res}$, rather than to the total field $E = |\vec{E}|$ (at very large energies, FLR corrections proportional to $|E_-|^2\, J_3^2(k_\perp v_\perp/\Omega)$ also play a role [5]; the two components $E_\pm$, in any case, enter in $D_2$ with very different weights). As well known, in the cyclotron frequency domain the ratio $E_+/E$ is sensitively dependent on the plasma composition and on the frequency ratio $\omega/\Omega$, although less so in the case of first harmonic heating than in minority heating scenarii.

5) First harmonic heating is a finite Larmor radius effect, so that for small to moderate energies $\hat{D}_2$ is proportional to the perpendicular energy of the heated ions. As a consequence, particles which begin acquiring energy will to be heated further more efficiently, and the process has a tendency to run away. Saturation through FLR effects begins only at perpendicular energies such that $k_\perp^2 v_\perp^2/\Omega_o^2 \gtrsim 10$. Since typically $k_\perp^2 v_{thi}^2/\Omega_o \simeq 0.1$ to 0.2, this corresponds to energies about 100 times thermal. Thus under normal conditions the heating rate is proportional to $\beta_i$: as mentioned in the introduction, the single transit absorption is often relatively low in an ohmic plasma, but boosts itself up if sufficient power is available to overcome the initial phase.

*2.3 – Quasilinear power balance and the evaluation of the quasilinear diffusion coefficient.* In dimensionless notations we can rewrite Eq. (21) as

$$\frac{1}{\nu_{ii}}\left(\frac{\partial F_i}{\partial t}\right)_{QL} = \frac{1}{w}\frac{\partial}{\partial w}\left(w\,\hat{D}_2\frac{\partial F_o}{\partial w}\right) \tag{23}$$

with $w = v_\perp/v_{thi}$ and

$$\hat{D}_2 = \frac{\Omega_o}{\nu_{ii}}\left(\frac{Ze}{2m\Omega_o v_{thi}}\right)^2\left(\frac{R}{r|\sin\vartheta_{Res}|}\right)\sum_{n_\varphi}\left|\mathrm{Re}\sum_{m_\vartheta} E_+(r,m_\vartheta,n_\varphi)\,e^{-ih_{res}}\,J_1(\mu w)\right|^2 \tag{24}$$

where $\mu = k_\perp v_{thi}/\Omega_o$. These equations allow in principle the construction of the quasilinear diffusion coefficient $D_2$ on each magnetic surface from the solution of the wave equations; they should therefore be regarded as the interface between wave codes and Fokker–Planck codes. As mentioned in the introduction, however, this evaluation is rather cumbersome, and seldom implemented. In addition to the heavy numerical burden that such a computation would represent, a serious consistency problem is likely to arises between the power balance of the wave code and that of the Fokker–Planck code.

The quasilinear heating rate can be evaluated using Eq. (23):

$$\begin{aligned} \dot{W} &= \frac{m_i}{2} \int v_\perp^2 \left( \frac{\partial F_i}{\partial t} \right)_{QL} d\vec{v} \\ &= -2\pi \nu_{ii}\, m_i v_{thi}^2 \int_{-\infty}^{+\infty} du \int_0^\infty w^2 \hat{D}_2(w) \frac{\partial F_i}{\partial w} dw \end{aligned} \tag{25}$$

(note that $\dot{W}$ does not depend on the collision frequency: the factor $\nu_{ii}$ cancels with the one in the denominator of the dimensionless definition of the diffusion coefficient $\hat{D}_2$). It can be shown [16] that

$$\dot{W} = \langle P_{abs} \rangle_\vartheta \tag{26}$$

where $P_{abs}$ is the power absorbed from the waves, and the average is over the magnetic surface; this equality is required for power conservation within the quasilinear approximation.

In practice, however, it is very difficult to obtain agreement between the power $P_{abs}$ evaluated with the wave code, and the heating rate $\dot{W}$ evaluated by the Fokker–Planck solver, because of internal cancellations in the inner sum in Eq. (23), and of the already mentioned sensitivity of $D_2$ to the details of the field polarization near resonance. More importantly, if, as it is practically always the case, the wave code solves the wave equations in the FLR approximation, agreement with a FP code based on Eq. (23), which is valid to all orders in the Larmor radius, cannot be expected even in principle. Thus, while strictly speaking Eq. (26) should be regarded as an independent consistency check, in practice it is always used to *renormalize* the diffusion coefficient $D_2$ so that power conservation is satisfied.

In most cases, the quasilinear diffusion coefficient can be further simplified by rewriting it *as if only a single plane wave were present*:

$$\hat{D}_2(w) = D_{QL}\, J_1^2(\xi w) \qquad \xi = \frac{k_\perp v_{thi}}{\Omega_o} \quad w = \frac{v_\perp}{v_{thi}} \tag{27}$$

The constant $D_{QL}$ can be conveniently chosen by specifying the *initial* heating rate, i.e. the heating rate $\dot{W}_M$ for the Maxwellian plasma at the temperature $T_i$ before heating begins. From (24)

$$\dot{W}_M = 4\,\nu_{ii}\,D_{QL}\,n_i T_i \int_0^\infty w^3 J_1^2(\xi w)\, e^{-w^2}\, dw \tag{28}$$

This way of normalizing $\hat{D}_2$ has also the advantage that $\dot{W}_M$ is a quantity directly accessible experimentally, from the slope of the energy content at the beginning of the heating pulse. If FLR effects can be neglected, one can further simplify

$$\hat{D}_2(w) \simeq \frac{1}{2}\xi^2 w^2 \tag{29}$$

and the equation for $D_{QL}$ reduces to

$$\nu_{ii}\,D_{QL} = \frac{\dot{W}_M}{8\,n_i T_i\,\xi^2} \tag{30}$$

The use of Eq. (27) is well justified even for quite broad launched spectra, since for the fast wave both $k_\perp$ and the polarization depend only weakly on the parallel wavevector component $k_\parallel$ [1]. This is illustrated for the ASDEX Upgrade case in figs. 2 and 3. In fig. 5 we compare $\hat{D}_2$ evaluated for a single plane wave with $\hat{D}_2$ evaluated for the nominal spectra (shown in fig. 4) of the ASDEX Upgrade antenna in the symmetric and antisymmetric configurations [17]. The effect of spectral broadening on $\hat{D}_2$ is completely negligible for $k_\perp v_\perp/\Omega_o \lesssim 5$ to 10, and not very significant even above: for ions reaching such high energies, as mentioned above, inaccuracies due to the surface averaging procedure are probably larger than the difference between the three curves in fig. 5. At larger $\beta_i$ the influence of the launched spectre on $\hat{D}_2$ tend to be even smaller.

We conclude that Eq. (27), with $k_\perp^2$ evaluated for $k_\parallel = 0$, is fully adequate for most purposes. This simplifies drastically coupling a Fokker–Planck codes to a full wave code: essentially no other information but the power deposition profile needs to flow from latter to the former.

## 3 – Approximate solution of the quasilinear equation in the moderate power approximation.

It is clearly out of question to solve the quasilinear equation analytically in two dimensions. If the applied power is not too large (according to a criterion which will be specified later), however, we can as a first approximation simplify the kinetic equation by neglecting the anisotropy which develops in the ion distribution function because IC heating fuels mainly the perpendicular degree of freedom. This approach was successfully applied by Stix to the case of minority heating [4]. Of course, the distribution of fast ions will be rather anisotropic also in the case of first harmonic heating (possibly more than in the minority case); the number of such ions, however, will be relatively small, so that the anisotropy will not influence appreciably the overall power balance and the propagation and absorption of the waves.

As a preliminary justification of the moderate power approximation, let us estimate the average heating rate $\dot{W} = P/V_{eff}$ assuming that the effective volume $V_{eff}$ is within the inner quart of the plasma radius. With the parameters of table 1 (including the appropriate elongation factor) we obtain

$$\begin{aligned} \dot{W}_{AUG} &\simeq 1.3\,P \qquad \text{for ASDEX Upgrade} \\ \dot{W}_{ITER} &\simeq 0.013\,P \qquad \text{for ITER} \end{aligned} \tag{30}$$

($P$ in MW, $\dot{W}$ in W/cm$^3$ = MW/m$^3$). Thus the local heating rate can reach a few W/cm$^3$ in ASDEX Upgrade (with an installed h.f. power of 4 MW), and perhaps 0.5 W/cm$^3$ in ITER. As will be seen below, the dimensionless quasilinear diffusion coefficient is at most of order unity at these power density levels in the relevant range of energies. In this respect the situation is different than in the case of minority heating, since the absorbed power is available to all ions or a large fraction thereof, rather than to a small minority.

The dimensionless steady state kinetic equation for the isotropic part of the ion distribution function (without losses) is of the form:

$$\frac{1}{F_o}\frac{dF_o}{dv} = -2v\frac{B(v)}{A(v)} \tag{31}$$

with

$$\begin{aligned} A(v) &= \sum_\beta \frac{\nu^{i/\beta}}{\nu^{i/i}}\Psi(\gamma_{i\beta}v) + \bar{D}_2(v) \\ B(v) &= \sum_\beta \frac{\nu^{i/\beta}}{\nu^{i/i}}\frac{T_i}{T_\beta}\Psi(\gamma_{i\beta}v) \end{aligned} \tag{32}$$

where

$$\bar{D}_2(v) = D_{QL} \int_0^1 (1-\mu^2)\, J_1^2\left(\xi v (1-\mu^2)^{1/2}\right) d\mu \tag{33}$$

is the isotropic part of the quasilinear diffusion operator. Before solving Eq. (31), let us exhamine $\bar{D}_2(v)$ in some more detail.

The result of averaging $J_1^2(\xi w)$ over pitch angle is shown in fig. 6. Taking the isotropic part reduces somewhat the value of $D_2$ for small $k_\perp v_\perp/\Omega$, since

$$\frac{1}{4}\int_0^1 (1-\mu^2)\left(\xi v (1-\mu^2)^{1/2}\right)^2 d\mu = \frac{2}{15}\xi^2 v^2 \tag{34}$$

and smooths out the oscillations at very large Larmor radii. The last feature is easily explained by the finite range of perpendicular velocities which contribute to the integral at constant $v$. For analytic work the rather inconvenient exact expression (33) for $\bar{D}_2(v)$ might be conveniently approximated with a rational function of the form

$$\bar{D}_2(v) = \frac{2}{15} D_{QL} \frac{\xi^2 v^2}{1 + g(\xi^2 v^2)^k} \tag{35}$$

Imposing that the r.h. side should reproduce the asymptotic behaviour of the integral in Eq. (33), averaged over the oscillations of the Bessel function, gives $k = 3$ and $g = 4\pi/15$. This choice however excessively cuts the first peak of $\hat{D}_2(\xi v)$. A better choice could be $k = 4$ and $g = 1/10$, which is quite accurate up to the maximum, and interpolates reasonably well up to $\xi^2 v^2 \simeq 10$. The two approximations suggested here are shown as function of the normalized velocity in fig. 7.

In figs. 8 and 9 we have plotted the dimensionless diffusion coefficient $\hat{D}_2$ for ASDEX Upgrade and ITER at a power density of 1 W/cm$^{-3}$, versus the normalized velocity and versus energy, respectively. From the second representation we easily recognize that for our purposes, in any case, we do not need an accurate analysis of what happens at very large Larmor radii: Eq. (35) with $g = 0$ is already sufficient up to the largest energies which need to be considered. Noting that the peak of $J_1^2(x)$ occurs at $x \simeq 10$, the condition for the validity of the small Larmor radius approximation is that the energy of most ions should not exceed

$$E \ll 10\frac{m_i c^2}{n_\perp^2} = 9.38\frac{A_i}{10^{-3}\, n_\perp^2}\ \text{MeV} \tag{36}$$

(we recall that $10^{-3}\, n_\perp^2$ is of order unity for the Fast Wave in the ion cyclotron frequency range [1]). Note that this condition is independent from the temperature. Although of

course a few ions can reach higher energies, we can safely assume that their number will not be very large, particularly in ASDEX Upgrade, where they are not well confined.

From fig. 9 we also learn that $D_2$ is at most of order unity in this energy range, as already anticipated. A sufficient condition for the validity of the moderate power approximation is that $D_2$ should exceed unity, if at all, only at energies much greater than thermal. This condition can be written

$$D_{QL}\,\xi^2 \ll 1 \tag{37}$$

When it is satisfied the distribution function is already decreased by several orders of magnitude before a true suprathermal tail develops. The tail is then relatively thin, so that the isotropic approximation, which is certainly not valid, does not greatly influence global properties which depend on moments of the distribution function. Condition (37) is well satisfied in both ASDEX Upgrade and ITER. We conclude that the moderate power approximation is practically always justified if FHIC heating is applied alone. FHIC heating on the other hand could be rather sensitive to synergetic effects with other heating methods, particularly neutral beam injection [18] and minority heating [19], which by themselves produce suprathermal ions; the investigation of these effects however exceeds the scope of the present analytic approach.

Although in the case of FHIC heating Eq. (31) cannot be solved in closed form even using Stix approximations for the coefficients of the collision operator, it is trivially integrated numerically. A few results are shown in fig. 10 for $\dot{W} = 1$ W/cm$^{-3}$ at various temperatures for both ASDEX Upgrade and ITER, and in fig. 11 for different heating rates in ASDEX Upgrade starting from an ohmic temperature of 2 keV. While deviations from Maxwellian are clearly visible, a look to the vertical scale confirms that the suprathermal tail is relatively thinly populated even at the highest temperatures and heating rates. The same conclusion follows from fig. 12, which shows the average energy $T_{eff}$ in the quasilinear distribution function versus the initial heating rate for an initial background temperature of 2 keV in ASDEX Upgrade. $T_{eff}$ increases faster than linear with $\dot{W}$; $\Delta T$ however remains modest, reaching 0.5 keV at $\dot{W} \simeq 1.5$ W/cm$^{-3}$. In fig. 12 we also show the ion energy at which $D_2(u)$ reaches unity: when $\dot{W}$ exceeds about 1.5 W/cm$^{-3}$ this energy becomes comparable to the initial thermal energy, and the number suprathermal particles can be expected to increase rapidly. This power level can be regarded as the upper limit for the application of the moderate power approximation.

In ITER, because of the higher density and larger volume, about the same power is available per particle than in ASDEX Upgrade in spite of the much larger total installed

power; hence at low temperature first harmonic heating is relatively inefficient. Once a temperature of the order of 10 keV is reached, however, the suprathermal population appears sufficient to increase appreciably the efficiency over the ohmic level and to start the self–boosting effect of FHIC heating. We will discuss this effect and the influence of FHIC heating on the reactivity near ignition in the next section.

It should be clear that the distribution functions shown in figs. 10 and 11 are only illustrative. They are evaluated keeping both $\dot{W}$ and the background temperature in the collision operator constant, while on the one hand the heating rate evaluated for the "final" distribution is much higher than in the initial maxwellian situation, and on the other hand the temperature of the background plasma has also changed. It would not be difficult to iterate the procedure, reevaluating the quasilinear distribution function using the new values of $\dot{W}$ and of the effective temperature $T_{eff}$, and so on, until consistency is reached. This would make the run–away tendency of first harmonic heating even more evident: for example, the "final" average energy $T_{eff}$ would increase faster than quadratically as a function of the initial value of $\dot{W}$. The consistency reached with such a procedure, however, would be purely illusory. In practice, heating is performed at constant total power. This does not mean constant $\dot{W}$ either, since the increase of ion cyclotron damping due to the larger power available per ion, for example, will shift the balance between between direct ion and electron heating in favor of the former. It is clear however that $\dot{W}$ cannot increase beyond a certain limit if the total power is kept constant.

## 4 – Two dimensional solution of the quasilinear kinetic equation.

*4.1 – Legendre polynomials representation of the quasilinear operator.* Although it is commonly accepted that the one–dimensional quasilinear Fokker–Planck model gives a fair first approximation at low to moderate power levels, it is clearly desirable to test its validity by comparison with solutions of the full two–dimensional equation. Moreover, to evaluate the effects of quasilinear distorsions of the distribution function on wave propagation and on the stability of the plasma, it is necessary to have at least an estimate of the anisotropy of the suprathermal ion tail. It is surprisingly difficult to make such an estimate analytically, and to our knowledge none is available in the literature. The required information is therefore usually obtained using a fully two–dimensional bounce averaged Fokker–Planck solver [20]. In particular, only such a code can properly take into account the pitch–angle dependence of the quasilinear diffusion coefficient due to particle trapping in tokamaks, which becomes important

at large energies. Unfortunately, this approach is very time consuming, and can only occasionally be used to test simpler models.

If one accepts to neglect ion trapping effects, however, an intermediate approach is possible, based on the expansion of the distribution function of the heated ions in Legendre polynomials in the pitch–angle variable. This expansion is the natural generalization of the isotropic assumption made in the elementary analytic theory; if only the steady–state solution is required, it transforms the two–dimentional partial differential (1) into a system of ordinary differential equations whose numerical solution is only slightly more demanding that the integration of Eq. (31). Although valid only up to moderate ion energies, this approach is able to provide all the information relevant for a self–consistent description of IC heating, at a cost which is a small fraction of the full bounce–averaged treatment including trapping.

We therefore develop $f^i$ in Legendre polynomials

$$f^i(v,\mu,t) = \sum_n F_n(v,t)\, P_n(\mu) \tag{38}$$

Inserting this expansion into the collisional operator gives

$$\frac{1}{\nu_i}\frac{\partial F_n}{\partial t}\Big)_{coll} = \frac{1}{v^2}\frac{\partial}{\partial v} v^2 \left[\frac{\Psi_c(v)}{2v}\frac{\partial F_n}{\partial v} + \Psi_\tau(v) F_n\right] - n(n+1)\,\frac{\Theta_c(v)}{2v^3}\,F_n \tag{39}$$

where

$$\begin{aligned}
\Psi_c(v) &= \sum_\beta \frac{\nu^{i/\beta}}{\nu_i}\Psi(\gamma_{i\beta}v) \\
\Psi_\tau(v) &= \sum_\beta \frac{\nu^{i/\beta}}{\nu_i}\frac{T_i}{T_\beta}\Psi(\gamma_{i\beta}v) \\
\Theta_c(v) &= \sum_\beta \frac{\nu^{i/\beta}}{\nu_i}\Theta(\gamma_{i\beta}v)
\end{aligned} \tag{40}$$

The quasilinear diffusion operator is easily written in $v$, $\mu$ coordinates by using the identities

$$\begin{aligned}
w\frac{\partial}{\partial w} &= (1-\mu^2)\left(v\frac{\partial}{\partial v} - \mu\frac{\partial}{\partial \mu}\right) \\
\frac{1}{w}\frac{\partial}{\partial w} &= \frac{1}{v^2}\left(\frac{\partial}{\partial v}\cdot v - \frac{\partial}{\partial \mu}\cdot \mu\right)
\end{aligned} \tag{41}$$

Thus

$$\frac{1}{\nu_i}\frac{\partial f^i}{\partial t}\Big)_{QL} = \left\{\frac{1-\mu^2}{v^2}\frac{\partial}{\partial v}\left[v\,D\left(v\frac{\partial f^i}{\partial v} - \mu\frac{\partial f^i}{\partial \mu}\right)\right]\right. \\ \left. - \frac{1}{v^2}\frac{\partial}{\partial \mu}\left[\mu(1-\mu^2)\,D\left(v\frac{\partial f^i}{\partial v} - \mu\frac{\partial f^i}{\partial \mu}\right)\right]\right\} \tag{42}$$

The key for the success of the Legendre polynomial expansion is a suitable representation of the quasilinear diffusion coefficient (27), obtained using the multiplication theorem for Bessel functions

$$J_n\left(\xi_\perp v\sqrt{1-\mu^2}\right) = (1-\mu^2)^{n/2}\sum_{k=0}^{\infty}\frac{\mu^{2k}}{k!}\left(\frac{\xi_\perp v}{2}\right)^k J_{n+k}(\xi_\perp v) \tag{43}$$

Using this in Eq. (26) gives

$$\tilde{D}(v,\mu) = D_{ql}\,(1-\mu^2)^p\sum_{k=0}^{\infty}\mathcal{J}_k^p(v)\,\mu^{2k} \tag{44}$$

where we have introduced the functions

$$\mathcal{J}_k^p(v) = \left(\frac{\xi_\perp v}{2}\right)^k\sum_{k'=0}^{k}\frac{1}{k'!(k-k')!}J_{p+k'}(\xi_\perp v)J_{p+k-k'}(\xi_\perp v) \tag{45}$$

Here $p=0$ for fundamental cyclotron heating (minority heating) and $p=1$ in the present case of first harmonic heating. For each $v$ Eq. (44) is a Taylor expansion around the exact value of $\tilde{D}$ for $\mu=0$ (perpendicular velocity). Indeed, for $\mu=0$ it reduces to

$$\tilde{D}(v,0) = D_{QL}\,J_1^2(\xi_\perp v) \tag{46}$$

which is 'exact' to all orders in the Larmor radius. On the other hand, the series for $\mu\neq 0$ also looks like an expansion in the Larmor radius, since the $k$–th term begins as $(\xi_\perp v)^{2k+p}/k!$. The series therefore converges very rapidly for $\xi_\perp v \lesssim 1$. If $\xi_\perp v \gg 1$, on the other hand, there is increasing internal cancellation among the lower order terms; hence, although convergent everywhere, Eq. (43) can be used in practice only for values of $\xi_\perp v$ not exceeding a few units. As we have shown in the previous section, however, this is fully sufficient for our purposes. The first few functions $\mathcal{J}_k^p(v)$ for $p=1$ are shown in fig. 13.

The rapid convergence of the representation of the quasilinear diffusion coefficient based on Eq. (43) does not by itself guarantee the convergence of the Legendre expansion (38), of course. The advantage of using (43) instead of a power expansion of the

Bessel function is that at moderate energies it guarantees a rapid convergence of (38) for nearly perpendicular velocities, where it is most important, and confines possible convergence problems to nearly parallel velocities, where there are much less particles. A straightforward Larmor radius expansion of $\hat{D}$ [5], although giving a somewhat simpler form to the quasilinear operator, localizes the worst convergence problems of the Legendre expansion near perpendicular velocities, and therefore becomes useless already at much lower energies (of course, this problem arises only when the expansion is used in conjunction with the Ansatz (38), not in fully 2-dimensional Fokker Planck solvers).

Substituting (38) and (45) into the quasilinear operator we obtain

$$\begin{aligned}\frac{1}{\nu_i}\frac{\partial F_n}{\partial t}\Big)_{QL} = \left(n+\frac{1}{2}\right)\sum_m \Bigg\{ & \frac{1}{v^2}\frac{\partial}{\partial v}\left(v^2 \mathcal{D}^p_{00}(n,m,v)\frac{\partial F_m}{\partial v}\right) \\ & - \frac{1}{v^2}\frac{\partial}{\partial v}\left(v\,\mathcal{D}^p_{01}(n,m,v)\,F_m\right) + \frac{\mathcal{D}^p_{10}(n,m,v)}{v}\frac{\partial F_m}{\partial v} - \frac{\mathcal{D}^p_{11}(n,m,v)}{v^2}F_m \Bigg\}\end{aligned} \tag{47}$$

whith

$$\mathcal{D}^p_{ij}(n,m,v) = D_{ql}\sum_{k=0}^{\infty} Q^{p,k}_{ij}(2n,2m)\,\mathcal{D}^p_k(v) \tag{48}$$

where the coefficients $Q^{p,k}_{ij}$ are integrals over Legendre polynomials:

$$\begin{aligned} Q^{p,k}_{00}(n,m) &= \int_{-1}^{+1} P_n(\mu)\,(1-\mu^2)^{1+p}\,\mu^{2k}\,P_m(\mu)\,d\mu \\ Q^{p,k}_{01}(n,m) &= \int_{-1}^{+1} P_n(\mu)\,(1-\mu^2)^{1+p}\,\mu^{2k}\left(\mu\frac{\partial P_m}{\partial \mu}\right)d\mu \\ Q^{p,k}_{11}(n,m) &= \int_{-1}^{+1} \left(\mu\frac{\partial P_n}{\partial \mu}\right)(1-\mu^2)^{1+p}\,\mu^{2k}\left(\mu\frac{\partial P_m}{\partial \mu}\right)d\mu \end{aligned} \tag{49}$$

and

$$Q^{p,k}_{10}(n,m) = Q^{p,k}_{01}(m,n) \tag{50}$$

hence

$$\mathcal{D}^p_{10}(n,m,v) = \mathcal{D}^p_{01}(m,n,v) \tag{51}$$

Although it is possible to give analytic expressions for these integrals or to evaluate them numerically, both methods have disadvantages, particularly when high order polynomes are involved. We have found much more convenient to evaluate them using *Mathematica*.

For completeness, the general expression for the heating rate in the Legendre representation becomes

$$\begin{aligned}\frac{\dot{W}}{2\pi\nu_i m_i v_{thi}^2} &= -\int_0^\infty v^4\,dv \int_{-1}^{+1}(1-\mu^2)D(v,\mu)\left(v\frac{\partial F}{\partial v}-\mu\frac{\partial F}{\partial \mu}\right)d\mu \\ &= -\sum_{n=0}^{\infty}\sum_{k=0}^{\infty}\int_0^\infty v^4\,\mathcal{D}_p^k(v)\left\{H_p^k(n)v\frac{\partial F_n}{\partial v}-K_p^k(n)\,F_n(v)\right\}dv\end{aligned} \tag{52}$$

where

$$\begin{aligned}H_p^k(n) &= \int_{-1}^{+1}(1-\mu^2)^{1+p}\mu^{2k}P_n(\mu)\,d\mu = Q_{00}^{p,k}(n,0) \\ K_p^k(n) &= \int_{-1}^{+1}(1-\mu^2)^{1+p}\mu^{2k}\left(\mu\frac{\partial P_n}{\partial \mu}\right)d\mu = Q_{10}^{p,k}(n,0)\end{aligned} \tag{53}$$

Obviously, only the isotropic part $F_o$ contributes to the density and energy content.

*4.2 – Numerical implementation.* In the numerical implementation, the Legendre expansion was cut at the 20–th polynome, including only even terms in agreement with the symmetry of the problem. The resulting set of coupled ordinary differential equations

$$\frac{1}{\nu_i}\left\{\left(\frac{\partial F_n}{\partial t}\right)_{coll}+\left(\frac{\partial F_n}{\partial t}\right)_{QL}\right\}=0 \tag{54}$$

where the first term is given by (39) and the second by (47), has been integrated using finite elements for the discretization of the velocity variable. This method is particularly well suited to this problem, both because of its numerical efficiency, and because it makes particularly easy to impose the required boundary conditions.

The first step in the FEL discretization is to put (54) into weak variational form by requiring

$$0=\sum_m\int_0^\infty\left\{\frac{dG}{dv}\left(\mathcal{A}_{mn}\frac{dF_{2m}}{dv}+\mathcal{B}_{nm}F_{2m}\right)+G(v)\left(\mathcal{C}_{mn}\frac{dF_{2m}}{dv}+\mathcal{D}_{nm}F_{2m}\right)\right\} \tag{55}$$

for all $G(v)$ from an appropriate test function space. Here

$$\begin{aligned}\mathcal{A}_{mn} &= \frac{v}{2}\Psi_c(v)\,\delta_{nm}+\left(2n+\frac{1}{2}\right)v^2\mathcal{D}_{00}^p(2n,2m,v) \\ \mathcal{B}_{mn} &= v^2\,\Psi_\tau(v)\,\delta_{nm}-\left(2n+\frac{1}{2}\right)v\mathcal{D}_{10}^p(2n,2m,v) \\ \mathcal{C}_{mn} &= -\left(2n+\frac{1}{2}\right)v\mathcal{D}_{01}^p(2n,2m,v) \\ \mathcal{D}_{mn} &= 2n(2n+1)\frac{\Theta_c(v)}{2v}\,\delta_{nm}+\mathcal{D}_{11}^p(2n,2m,v)\end{aligned} \tag{56}$$

If the velocity integral is cut at a large but finite velocity $V$, one shold in principle add a boundary term arising from the integration by part of the terms containing second derivatives, and which represents the net flux of particles leaving the region of integration. In steady state this flux must vanish, hence the boundary term must be omitted. The only boundary condition to be explicitly imposed, therefore, pending normalization of the distribution function, is

$$F_0(0) = 1 \qquad F_{2n}(0) = 0 \quad \text{for } n \geq 1 \tag{57}$$

The discretization is performed using as test functions cubic hermite polynomials [21] localized on each mesh element.

*4.3 – Applications of the SSFPQL code to first harmonic ion cyclotron heating.* Figs. 14 to 16 show some examples of solution of the two dimensional steady state equations obtained with the SSFPQL code for the low density ASDEX Upgrade plasma already considered in the previous section. Fig. 14 a) is a logarithmic plot of the energy distribution at constant pitch–angle, such as it might be reconstructed from a charge–exchange diagnostic; fig. 14 b) shows a contour plot of the same distribution function in the $v_\parallel$–$v_\perp$ plane. These figures are made assuming an ohmic temperature of 2 keV for both ions and electrons, and a power absorption by the ions of 0.5 W/cm$^{-3}$. Figs. 15 and 16 plot the results of a power scan for the same plasma. At low power the effective temperatures versus $\dot{W}$ is identical to that obtained from the one–dimensional approximation, but the agreement is somewhat less satisfactory when $\dot{W}$ exceeds about 0.5 W/cm$^{-3}$.

As anticipated, at the power levels characteristic of FHIC heating the suprathermal ion tail is relatively weakly populated, although rather flat. At $\dot{W} = 1$ W/cm$^3$ the total energy content of the quasilinear distribution is only 0.35 keV per particle higher than in the ohmic plasma. On the other hand this energy is stored in an ion population with $k_\perp v_\perp / \Omega_c$ much greater than the thermal value; this is sufficient to boost the heating rate by 40% over the linear value The suprathermal tail is also very anisotropic, the increase in parallel energy being only about one fifth of the total energy increase.

A scan of the quasilinear modification of the heating efficiency of FHIC heating of the Tritium component in ITER versus the initial temperature is presented in figs. 17 and 18. According to these results, self–boosting of FHIC heating can be hoped only if the temperature of the ohmic plasma already reaches 8 to 10 keV. This conclusion might be somewhat pessimistic, however, since it is obtained at a constant power density, $\dot{W} = 0.5$ W/cm$^3$. Keeping in mind that at 20 keV a fraction of the order of 50% of

the power is absorbed by the electrons, this seems to be an upper limit for $\dot{W}$ near ignition. As the temperature decreases, however, the single–pass absorption by the electrons decreases faster than that of ions, so that the balance shifts in favor of the latter; thus somewhat higher values of $\dot{W}$ might be possible at ohmic temperatures. Moreover, the situation can be further improved by starting heating at a density lower than the the steady state value required during the ignited phase. It turns out on the other hand that altering the isotope composition of the plasma at a constant density has no favorable effect on FHIC heating. First harmonic heating of Deuterium is about 50% more efficient than FHIC heating of Tritium, as can be deduced by comparing figs. (19) and (20) with the previous ones.

These estimates are subject to the critics mentioned at the end of the previous section. To avoid misunderstandings, we also recall that the the quasilinear modifications of the distribution function and of the heating efficiency in a given target plasma discussed here establish themselves within a collision time from the beginning of the heating pulse. They should not be confused with the steady–state attainable after a sufficiently long heating period, of the order of the energy confinement time. To predict the evolution of the plasma on the latter, slower time scale, it is necessary to model the energy balance by including radial transport and losses. We do not try to quantify further these consideration here, since reliable conclusions can be reached only by using SSFPQL in conjunction with both a wave code and a tokamak transport code. We only wish to point out that SSFPQL offers a very efficient and flexible complement to such codes.

*4.4 – Quasilinear enhancement of the fusion reactivity.* Representing the distribution function as a sum of Legendre polynomes in the pitch–angle is also convenient in view of calculating the fusion reactivity, taking advantage of the algorithm suggested by Cordey et al. [22]. If, as in the present case, only one species (the heated one) deviates from a Maxwellian distribution, only the isotropic component of the distribution function of the heated species contributes to the reactivity, and the expression of Cordey et al. simplifies to

$$\langle \sigma v \rangle = \frac{8\pi^2}{n_a\, n_b} \int_0^\infty v^2\, dv\, F_o^a(v) \int_0^\infty v'^{\,2}\, dv'\, F_M^b(v) \int_{-1}^{+1} d\hat{\mu}\, \sigma(\hat{u})\, \hat{u} \tag{58}$$

where

$$\hat{u}^2 = v^2 + v'^{\,2} - 2vv'\hat{\mu} \tag{59}$$

('$a$' denotes the heated species, '$b$' the Maxwellian one).

Using this result, and values of the D–T reaction cross–section $\sigma(\hat{u})$ from [23], we have evaluated the fusion power density in the ITER Tritium FHIC heating case considered above, in the range $15 \leq T \leq 20$ (fig. 21). The quasilinear enhancement lies between 75% anf 50% (the relative enhancement decreases with increasing temperature). This is much larger than the relatively modest increase of the energy content, and is of course due to great weight of the suprathermal tail in $\langle \sigma v \rangle$. If it is not accompanied by a degradation of the confinement, the effect is sufficiently large to decrease the ignition temperature by several keV, and could reduce appreciably the minimum requirements on the installed h.f. power.

*4.5 – Analytic representation of the quasilinear distribution function.* In fig. 13, and in all similar plots obtained with SSFPQL, the difference between $F_i(v, \mu = 0)$ and the ohmic distribution function would be difficult to appreciate if the reference Maxwellian had not been plotted at the same time. This strong anisotropy suggests a simple analytic representation of the resulting ion distribution function, namely

$$F_i(u, w) = F_M(\gamma u)\, F_\perp(w) \tag{60}$$

where $F_M(\gamma u)$ is a maxwellian in the parallel velocity taking into account the increase in parallel energy through the factor $\gamma = (T/T_{\parallel,eff})^{1/2}$, and $F_\perp$ is the function obtained by integrating Eq. (31), but reinterpreted as the distribution of perpendicular velocities, and with the numerical value of $D_{QL}$ adjusted to reproduce the total energy content of the two–dimensional solution. The distribution function (60), in which the parallel and perpendicular velocity distributions are factorized, is particularly convenient for use in the investigation of wave propagation. Moreover, in the FLR approximation, the ion contribution to dielectric tensor is immediately expressed in terms of the Plasma Dispersion function [24] and the first two moments of the perpendicular part of the distribution function $F_\perp$.

**Conclusions.**

In this report the quasilinear modification of the ion distribution function during first harmonic ion cyclotron heating, and its effects on the heating rate and on the fusion reactivity, has been investigated both with a simple already well established analytic one–dimensional approach, and with a new two dimensional steady state solver of the quasilinear kinetic equation. By accepting to disregard trapped ion effects, the latter code has been made much faster than full surface–averaged codes, yet it can provide all the information required to study the influence of fast ions on wave propagation and

absorption. The insight gained in the derivation and discussion of this model can be used to build a selfconsistent description of this heating scenario which can be implemented with a reasonable numerical effort.

The examples presented in this report should be made quantitative by coupling modelling of FHIC heating with that of tokamak transport. Nevertheless, even in the present preliminary form, they allow a few interesting conclusions. The first is that success of FHIC heating of Tritium in ITER might require lowering somewhat the density of the target ohmic plasma; on the other hand, once started, the suprathermal tail produced by FHIC heating might lower the ignition temperature by a few keV, correspondingly reducing the power requirements. The second conclusion is that the conditions for FHIC heating in ASDEX Upgrade at intermediate density and power are sufficiently similar to those of ITER to make such an experiment particularly relevant.

TABLE 1

| | ASDEX U. | ITER (T) | (D) |
|---|---|---|---|
| Toroidal radius | 1.65 m | 7.75 m | |
| Plasma radius | 0.5 m | 2.25 m | |
| Magnetic field on axis | 2 T | 6 T | |
| Central density | $5\ 10^{19}$ m$^{-3}$ | $1.4\ 10^{20}$ m$^{-3}$ | |
| Central temperature | 2 to 5 keV | 5 to 20 keV | |
| Frequency | 60 Mhz | 60.1 Mhz | (91 Mhz) |

**References.**


[ 1] M. Brambilla, *Linear propagation and absorption of the fast wave near the first ion cyclotron harmonic*, Report IPP 5/52, August 1993.

[ 2] M. Brambilla, C. Hoffman, 20th EPS Conf. on Controlled Fusion and Plasma Physics, Lissabon 1993, Vol. III, p. 957.

[ 3] Killeen J., Kerbel G.D., McCoy M.G., Mirin A.A., *Computational methods for kinetic models of magnetically confined plasmas*, Springer, N.Y. 198?.

[ 4] Stix T.H., Nucl. Fus. **15** (1975) 737.

[ 5] Anderson D., Core W., Ericksson L.-G., Hamnén H., Hellsten T., Lisak M., Nucl. Fus. **27** (1987) 911.

[ 6] Anderson D., Eriksson L.-G., Lisak M., Plasma Phys. Contr. Fus. **29** (1987) 891.

[ 7] Hassan M.H.A., Hamza E.A., Phys. Rev. **E 48** (1993) 1359.

[ 8] Kennel C.F., Engelmann F., Phys. Fluids **9** (1966) 2377.

[ 9] Kasilov S.V., Pyatak A.I., Stepanov K.M., Nucl. Fus. **30** (1990) 2467.

[10] Becoulet A., Gambier D.J., Rax J.-M., Samain A., Proc. 8th Top. Conf. on Applications of RF Power to Plasmas, Irvine (CA., USA) 1989, p. 197.

[11] Helander P., Lisak M., Phys. Fluids **B 4** (1992) 1927.

[12] Kerbel G.D., McCoy M.G., Phys. Fluids **28** (1985) 3629.

[13] Catto P.J., Myra J.R., Phys. Fluids **B 4** (1992) 187.

[14] Cottrell G.A., Start D.F.H., Nucl. Fus. **31** (1991) 61.

[15] Kovanen M.A., Core W.G.F., J. Comp. Phys. **105** (1993) 14.

[16] Brambilla M., Kruecken T., Nucl. Fus. **28** (1988) 1813.

[17] Noterdaeme J.-M., Wesner F., Brambilla M., et al., Fus. Eng. Des. (1993), to be published.

[18] Van Eester D., Plasma Phys. Contr. Fus. **35** (1993) 441.

[19] Noterdaeme J.-M., Hoffmann C., Brambilla M., et al., Proc. 20th Europ. Conf. on Contr. Fusion and Plasma Phys., Lissabon, 1993, Vol. III p. 945.

[20] Karney C.F.F., Comp. Phys. Reports **4** (1986) 183.

[21] Appert K., Hellsten T., Vaclavik J., Villard L. Comp. Phys. Comm. **40** (1986) 73.

[22] Cordey J.G., Marx K.D., McCoy M.G., Mirin A.A., Rensink M.E., J. Comp. Phys. **28** (1978) 115.

[23] Bosch H.S., Review of data and formulas for fusion cross–sections, Report IPP I/252, 1990.

[24] Fried B.D., Conte S.D., *The plasma disperion function,* Academic Press, N.Y. 1961.

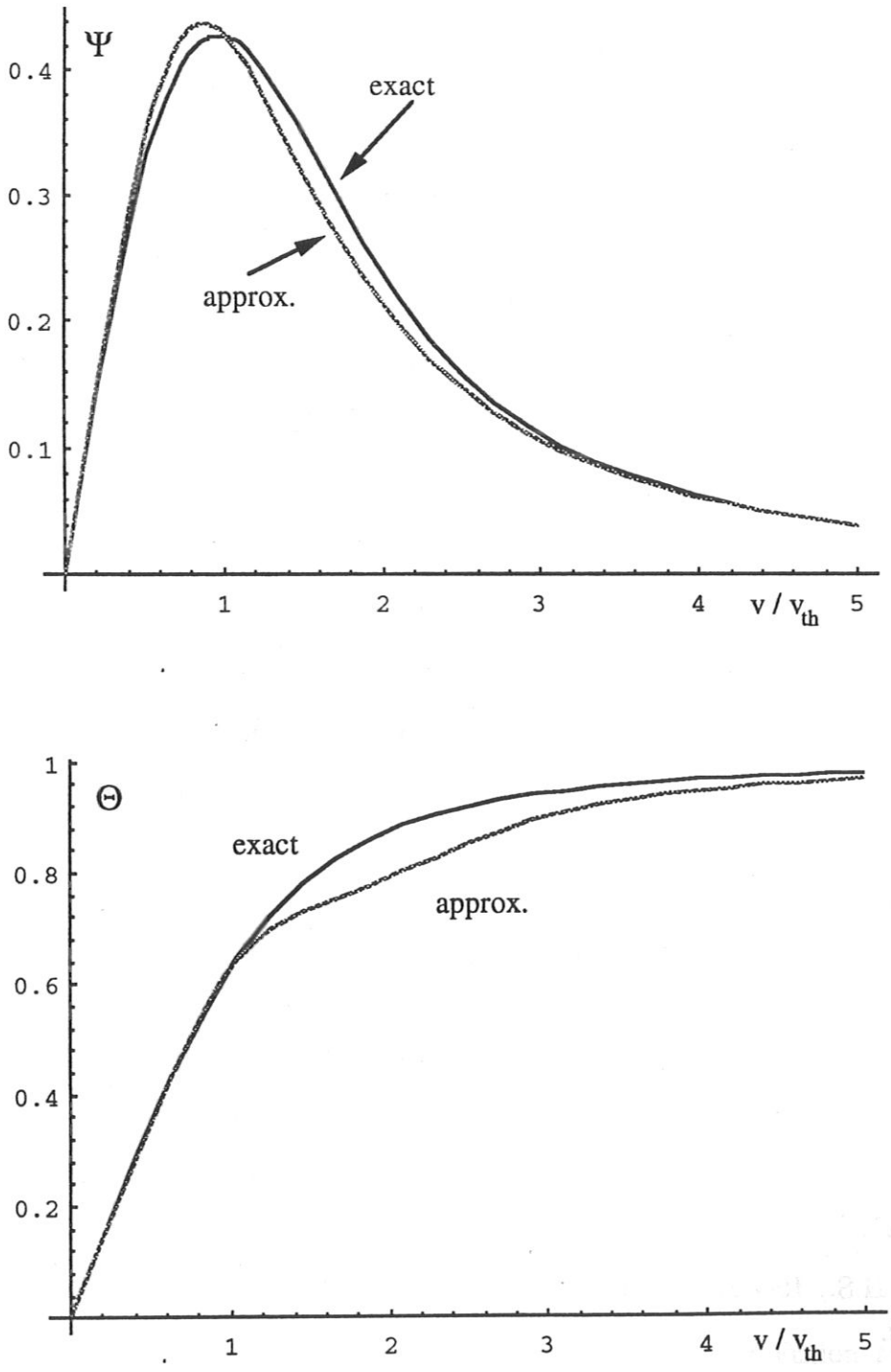


Fig. 1 - Stix approximations for the coefficients of the linearized Fokker-Planck collisional operator.

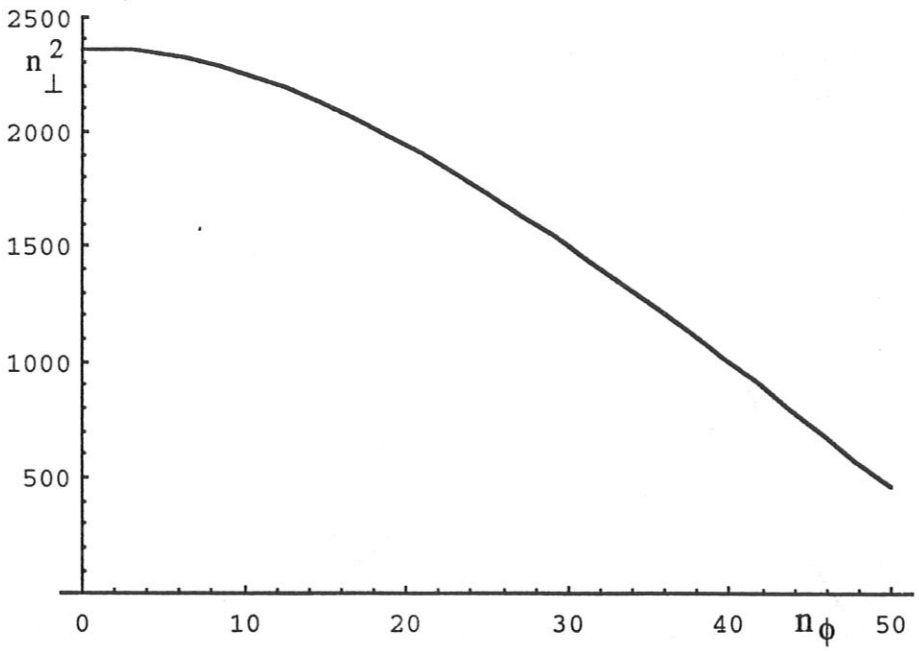


Fig. 2 - Perpendicular index squared versus $n_\phi$ ; ASDEX Upgrade, low density plasma.

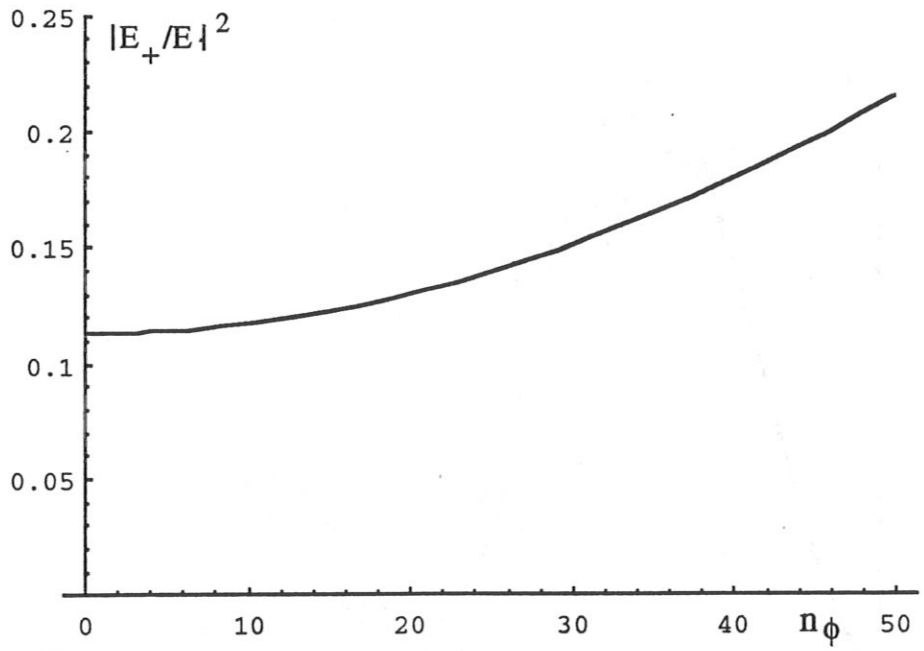


Fig. 3 - Polarization factor versus $n_\phi$ ; ASDEX Upgrade, low density plasma.

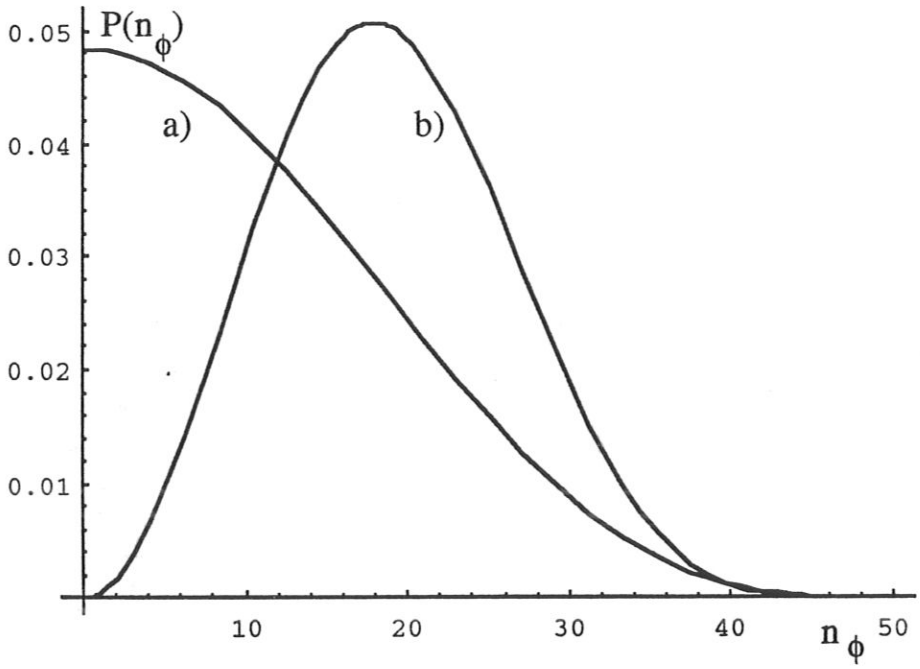


Fig. 4 - Power spectra for the symmetric (a) and antisymmetric (b) antenna configurations; ASDEX Upgrade low density plasma.

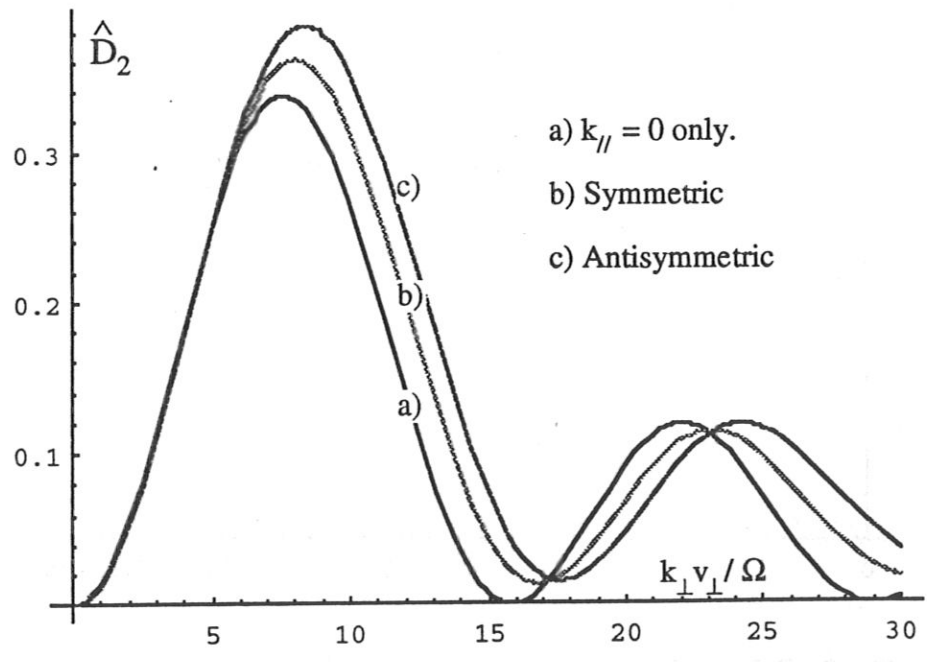


Fig. 5 - First harmonic heating quasilinear diffusion coefficient for the spectra of the ASDEX Ugrade antenna; low density plasma, plane stratified geometry.

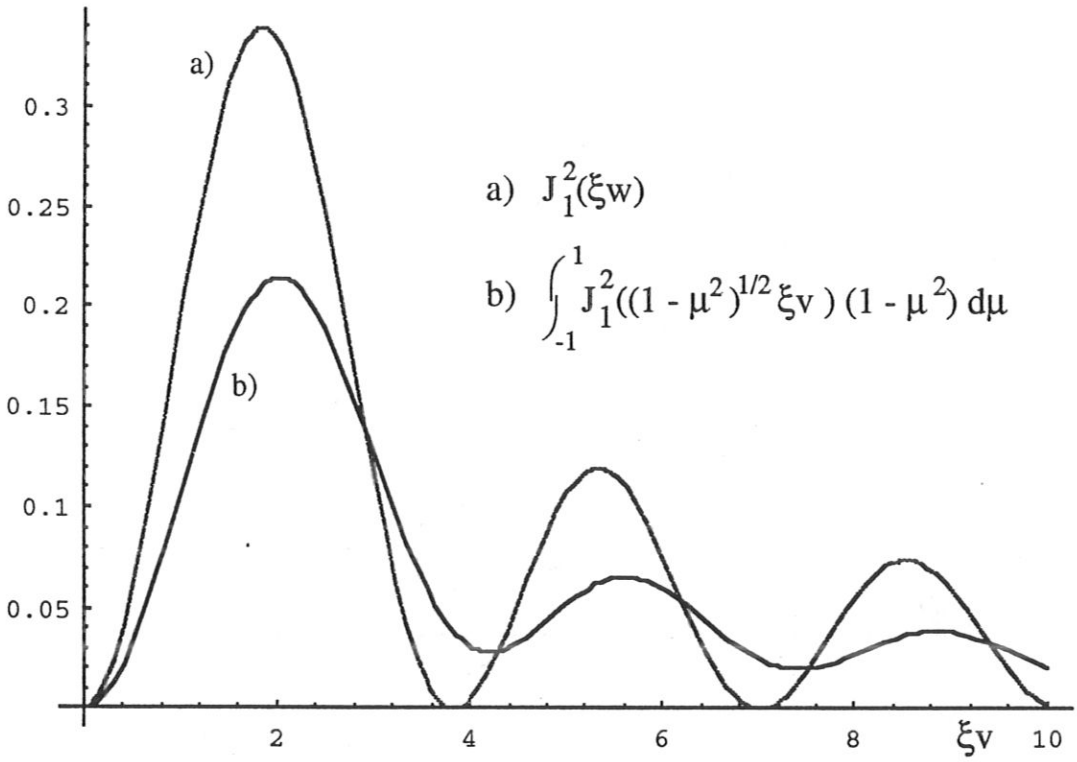


Fig.6 - The isotropic part of the quasilinear diffusion coefficient.

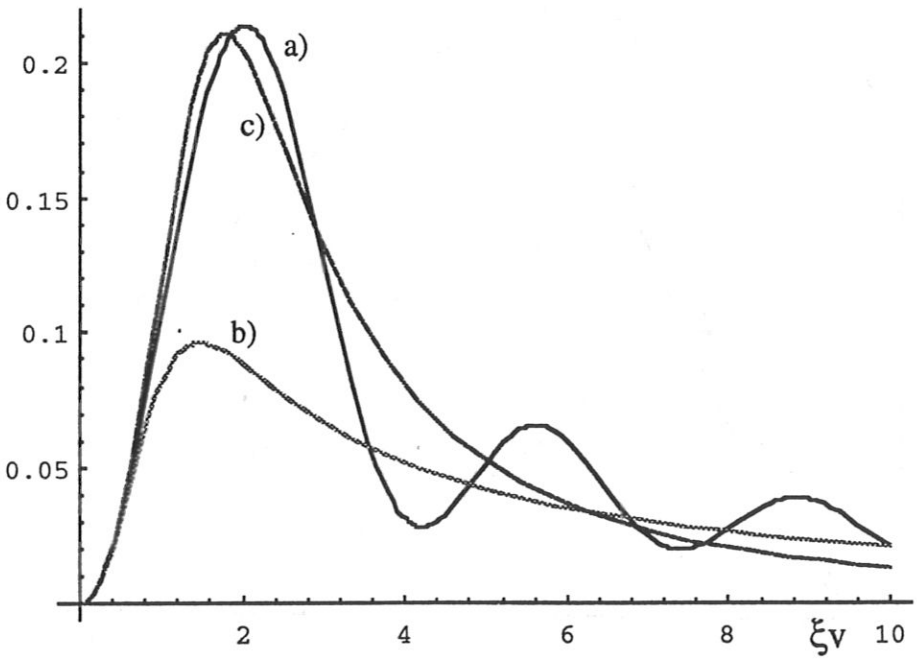


Fig. 7 - Interpolation of the isotropic part of the quasilinear diffusion coefficient.
a) Exact average of $J_1^2$ (ξw); b) Asymptotic behaviour $\sim 1/(\xi v)$;
c) Asymptotic behaviour $\sim 1/(\xi v)^2$

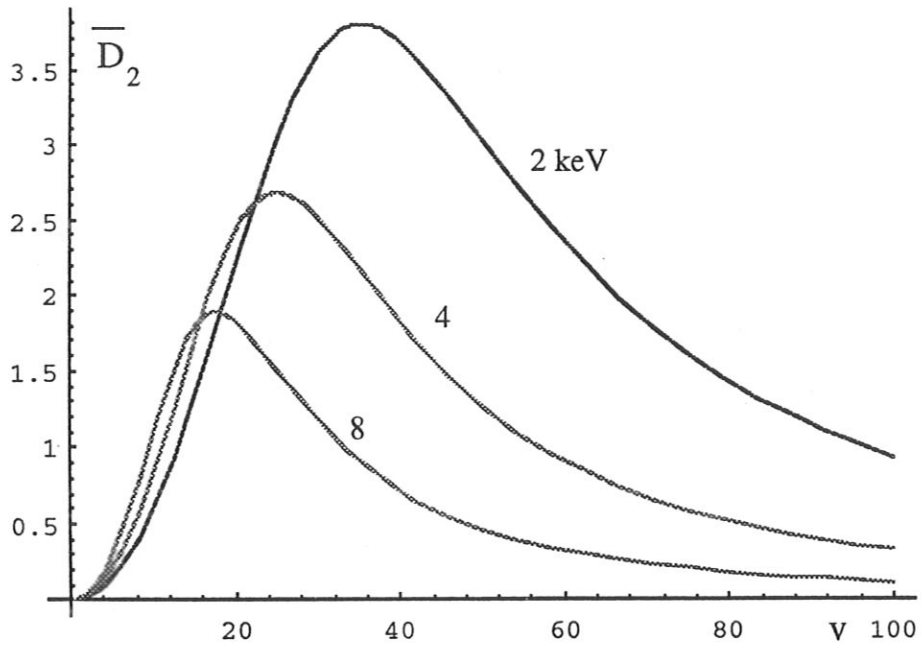


Fig. 8 - Isotropic part of the quasilinear diffusion coefficient at W = 1 W/cm$^3$,
a) ASDEX Upgrade plasma.

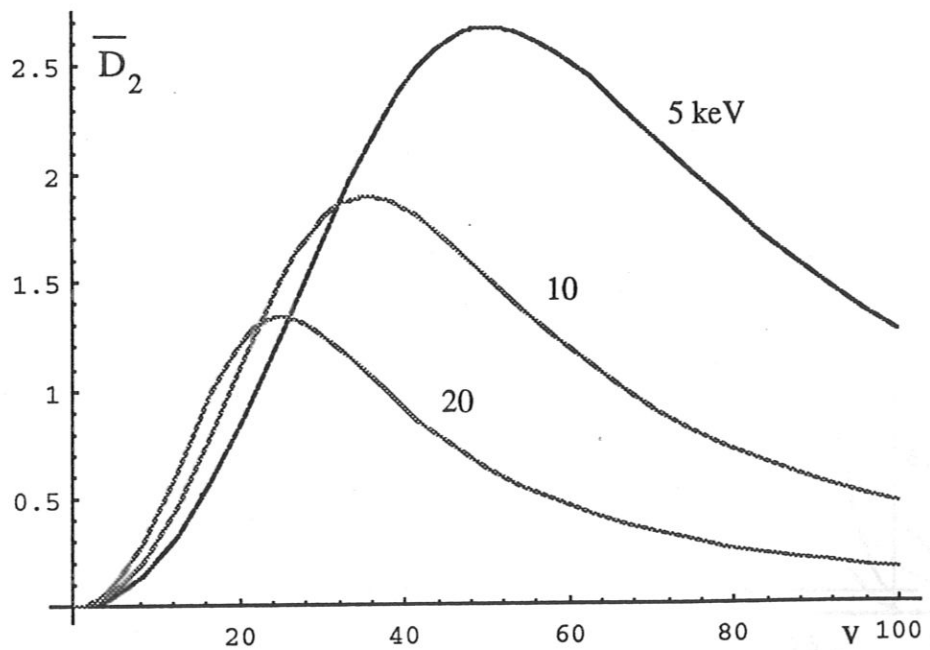


Fig. 8 - Isotropic part of the quasilinear diffusion coefficient at W = 1 W/cm$^3$,
b) ITER Tritium first harmonic heating.

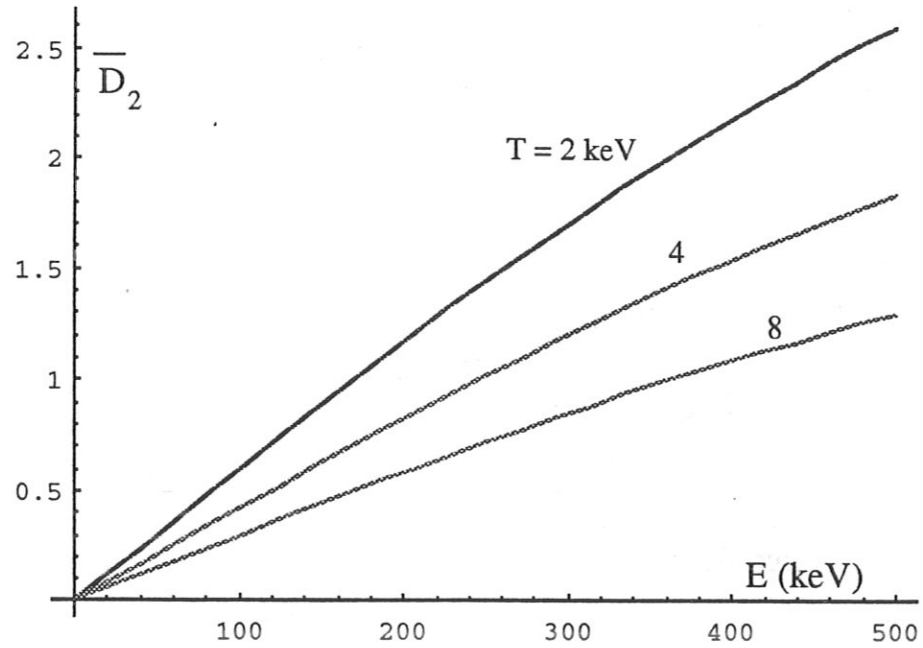


Fig. 9 - Isotropic part of the quasilinear diffusion coefficient versus energy, at W = 1 W/cm$^3$ . a) ASDEX Upgrade plasma.

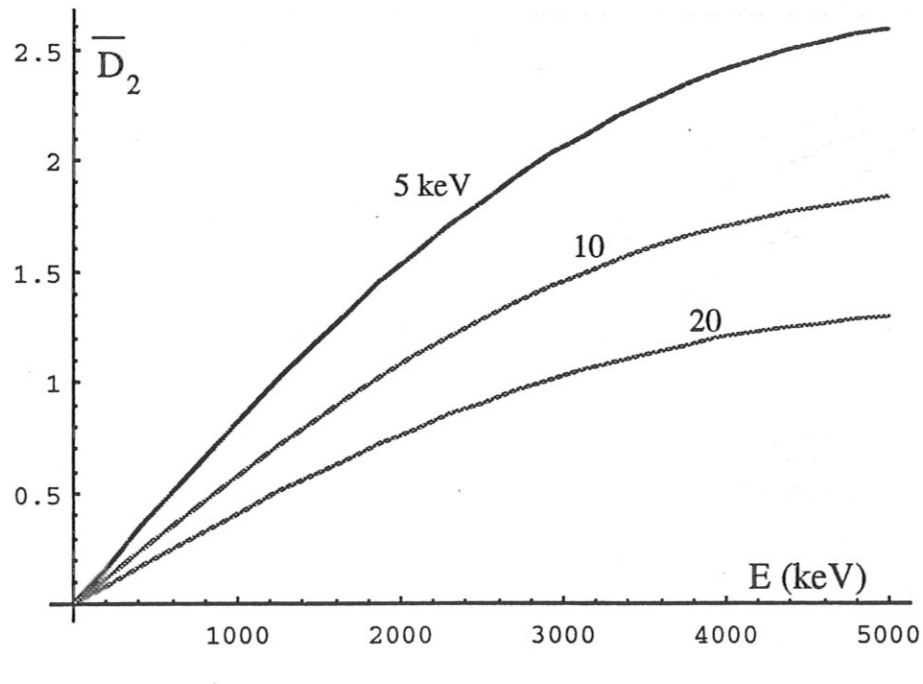


Fig. 9 - Isotropic part of the quasilinear diffusion coefficient versus energy, at W = 1 W/cm$^3$ . b) ITER Tritium first harmonic heating.

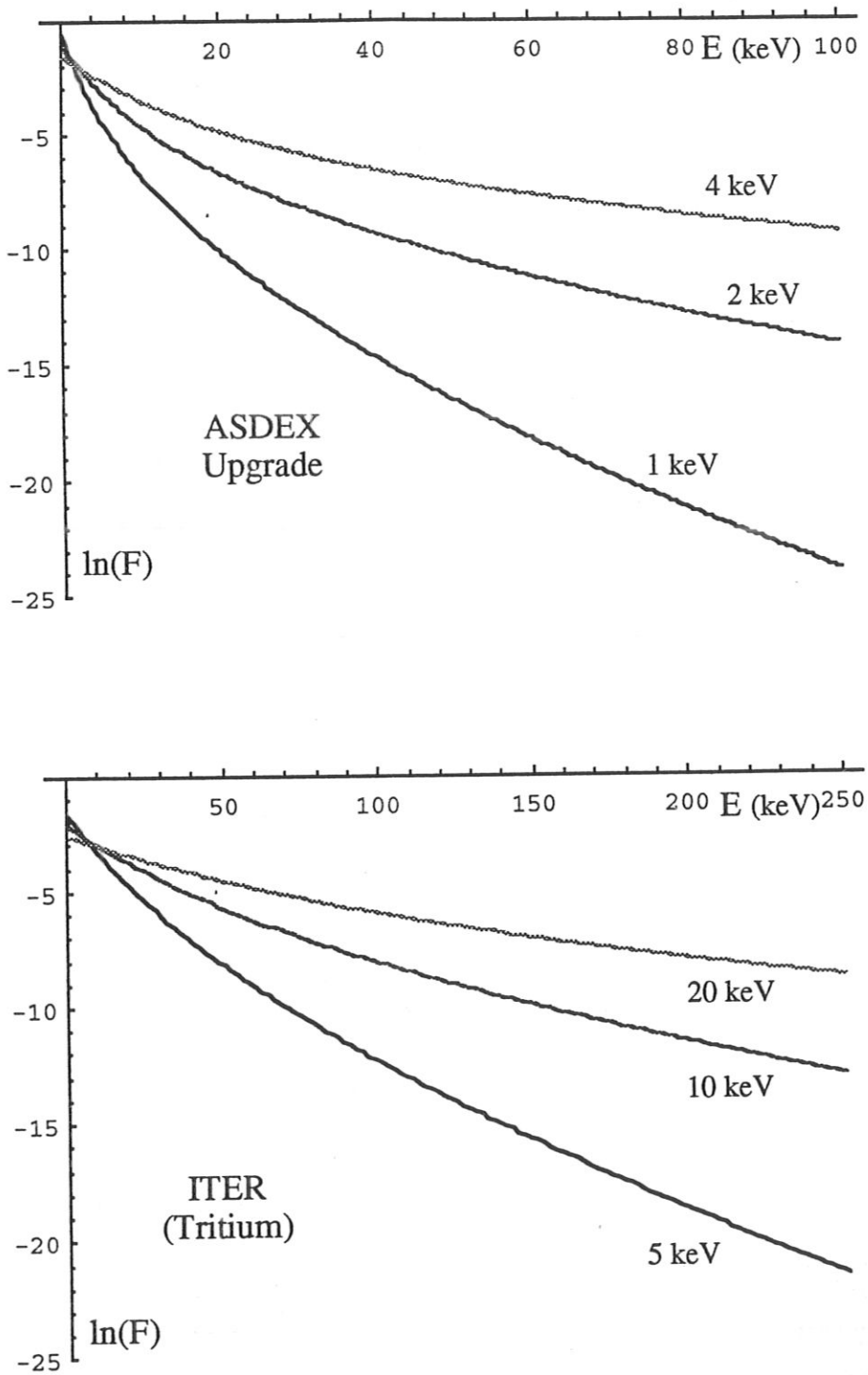


Fig. 10 - Isotropic part of the quasilinear distribution function at W = 1 W/cm$^3$ .
a) ASDEX Upgrade; b) ITER Tritium first harmonic.

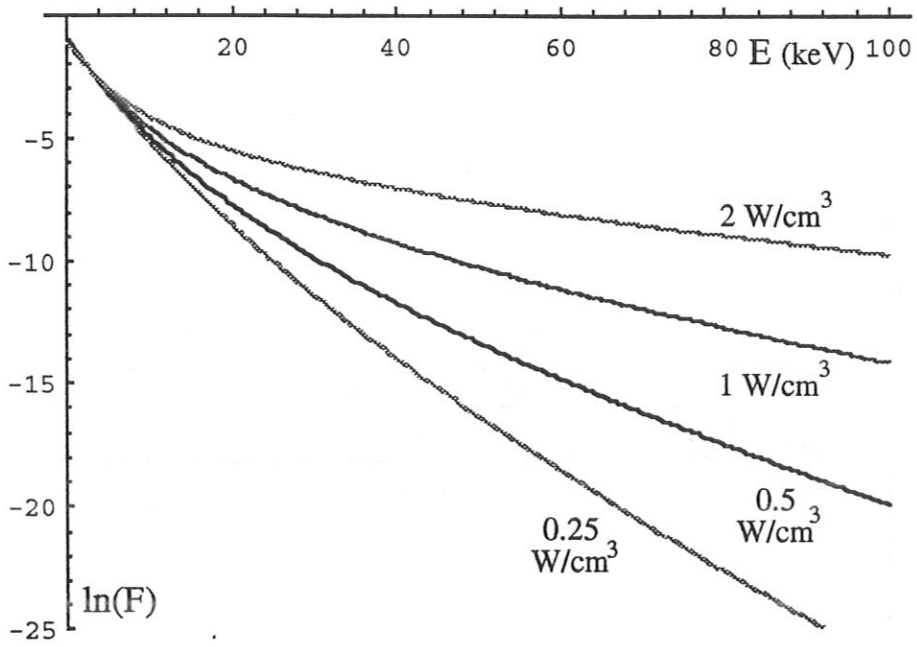


Fig. 11 - Isotropic part of the quasilinear distribution function at different power densities: ASDEX Upgrade, T = 2 keV.

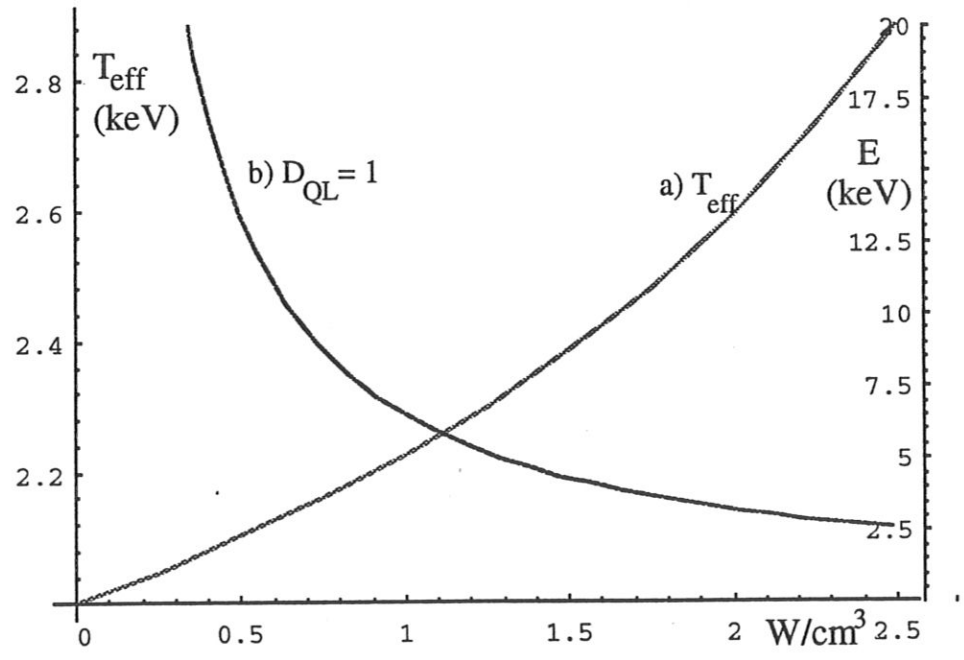


Fig. 12 - a) Average energy in the quasilinear distribution function versus initial heating rate. ASDEX Upgrade, initial temperatue 2 keV.
b) Energy at which $D_2(v) = 1$.

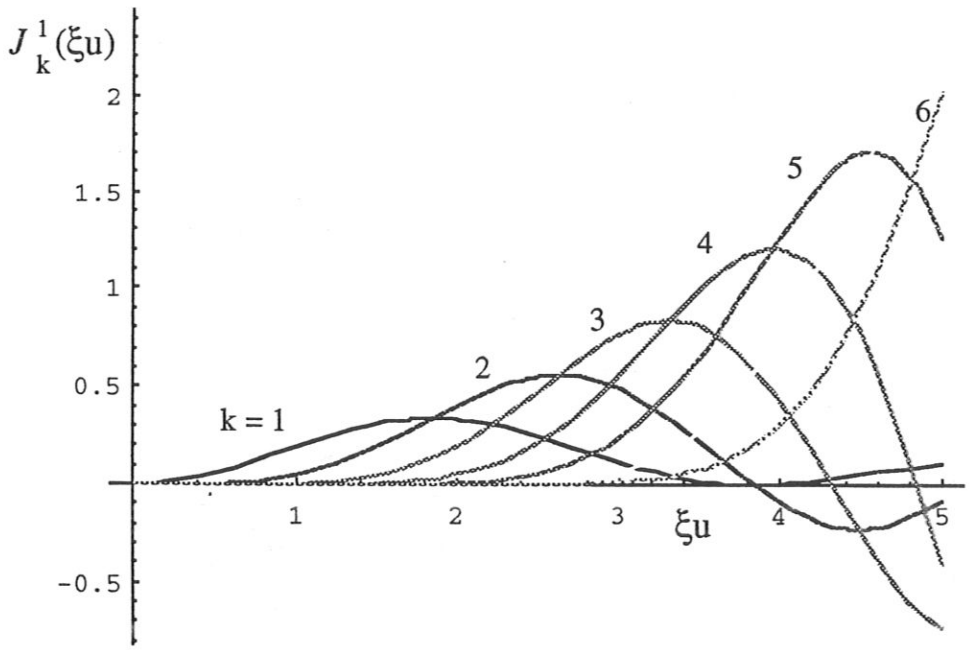


Fig. 13 - Coefficients in the Legendre-polynomial representation of the quasilinear diffusion coefficient for ICR first harmonic heating.

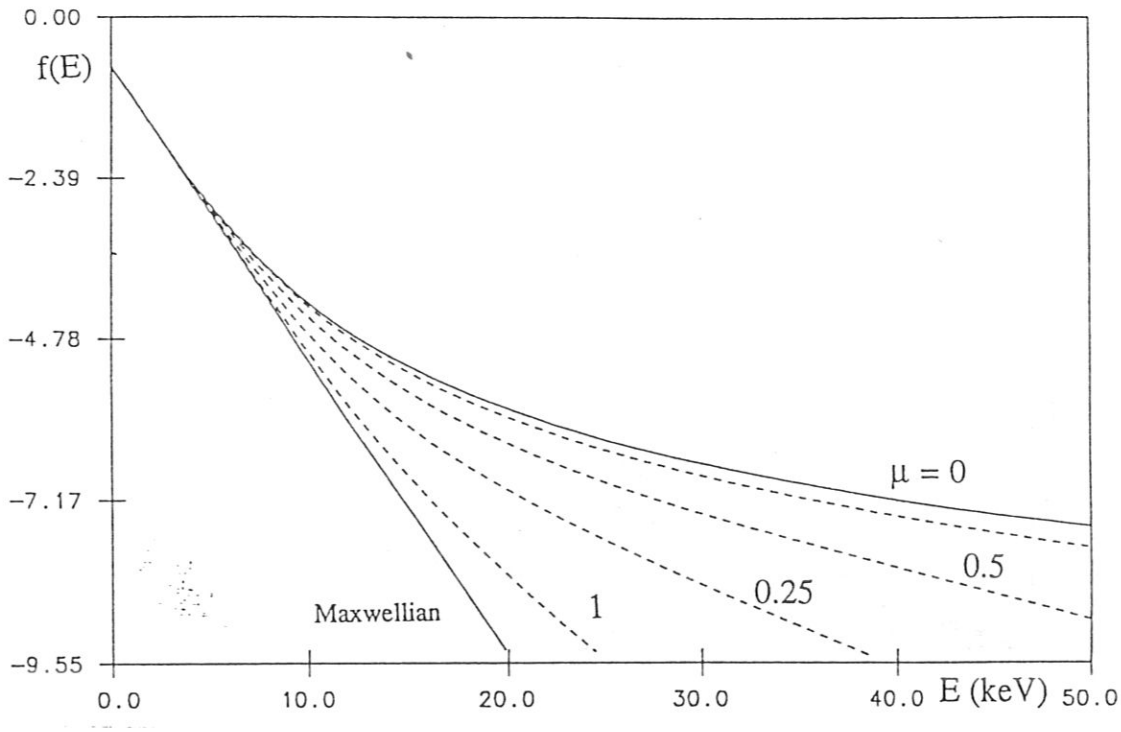


Fig. 14 a) - ASDEX Upgrade first harmonic heating (plasma parameters in Table 1), W = 0.5 W/cm$^3$. Distribution function at constant pitch-angle.

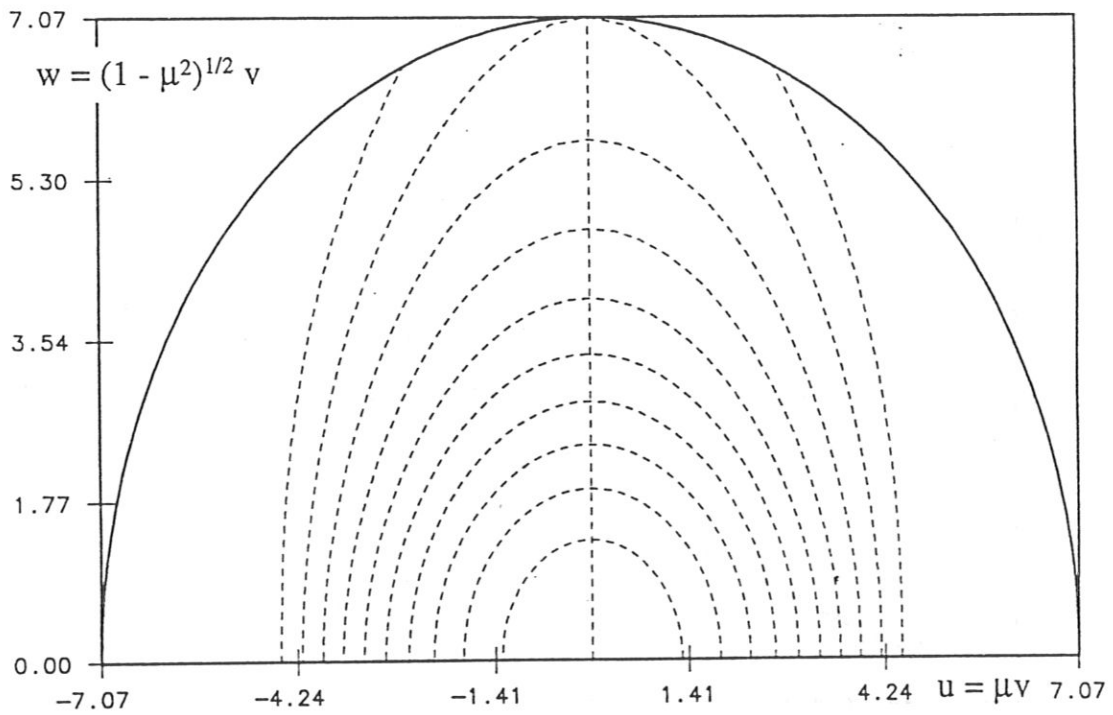


Fig. 14 b) - ASDEX Upgrade first harmonic heating (plasma parameters in Table 1), W = 0.5 W/cm$^3$. Contour plot of the ion distribution function (levels are in geometrical progression).

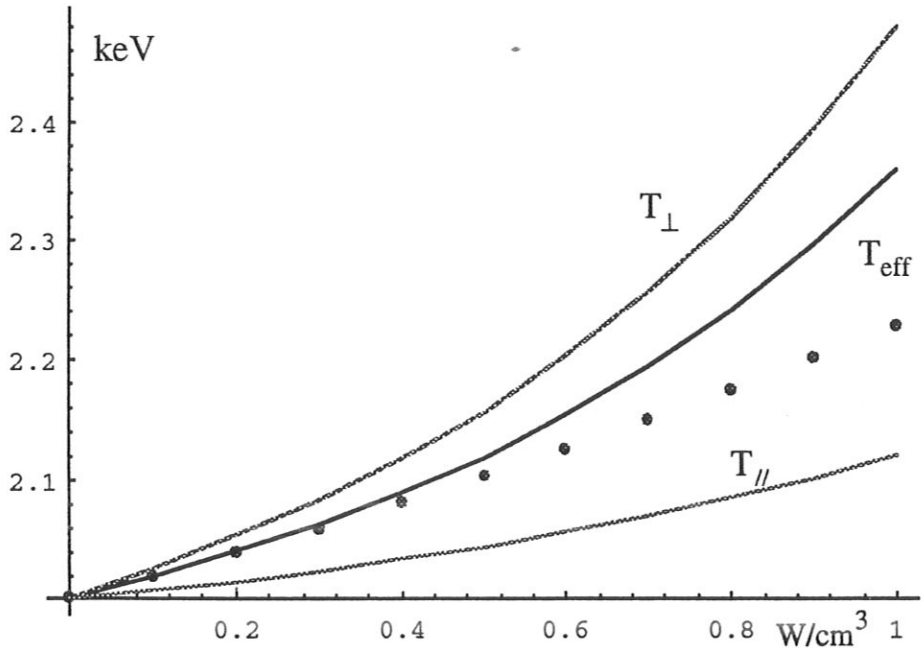


Fig. 15 - Effective temperature versus Heating Rate, ASDEX Upgrade first harmonic heating. The dots are the effective temperature predicted by the analytic one-dimesional model.

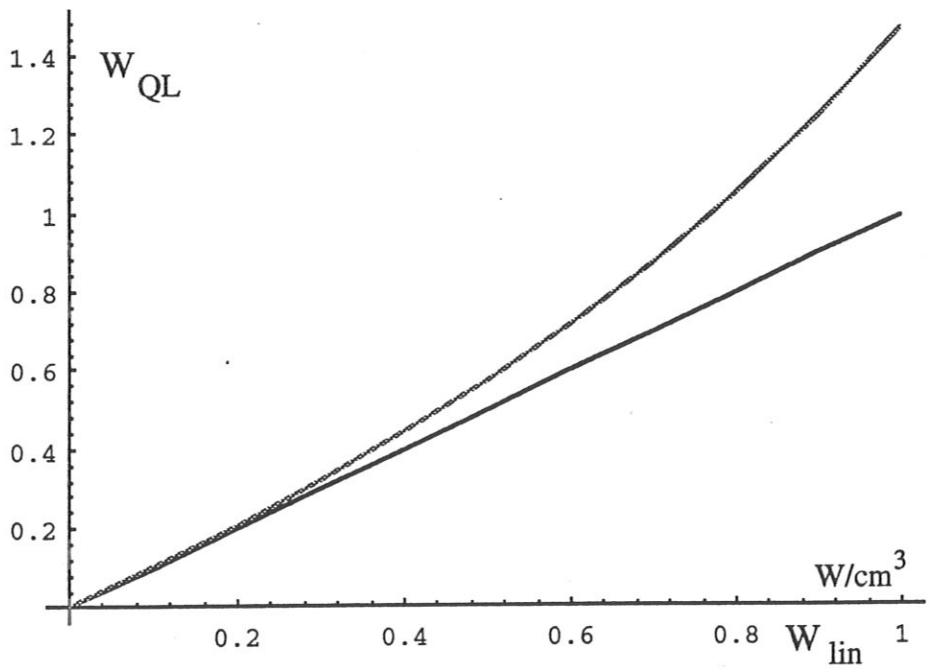


Fig. 16 -- Quasilinear vs linear heating rate, ASDEX Upgrade first harmonic heating.

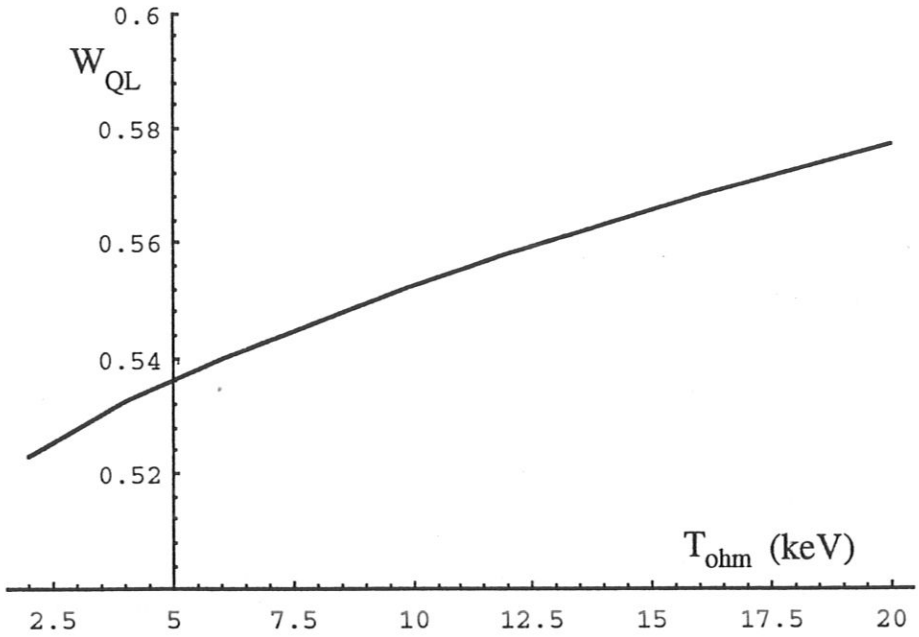


Fig. 17 - ITER first harmonic heating of Tritium (plasma parameters in Table 1); Quasilinear heating rate vs target plasma temperature for a linear rate of 0.5 W/cm$^3$.

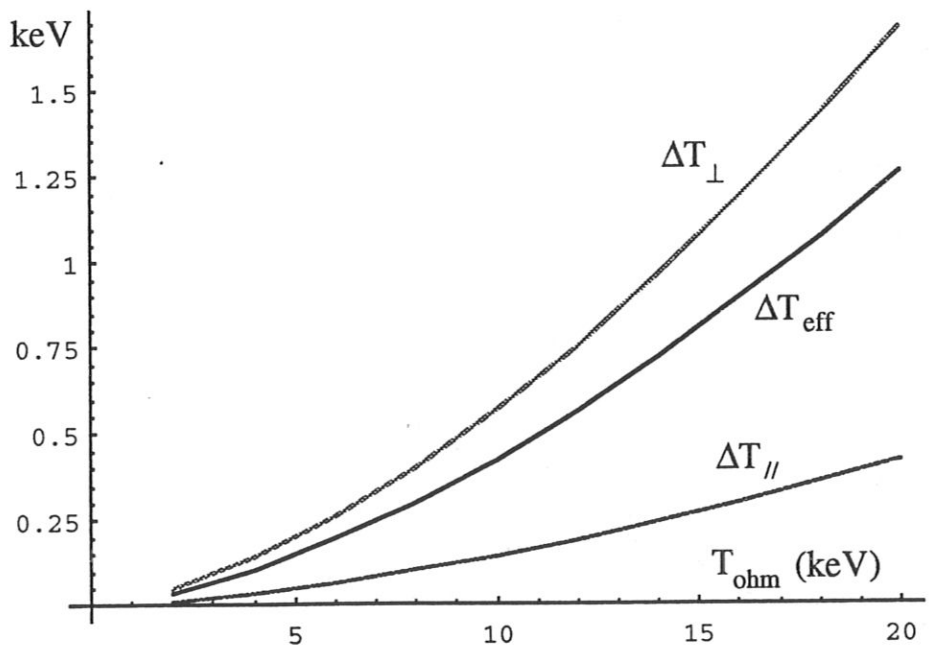


Fig. 18 - ITER first harmonic heating of Tritium (plasma parameters in Table 1); Quasilinear increase of the energy content vs target plasma temperature.

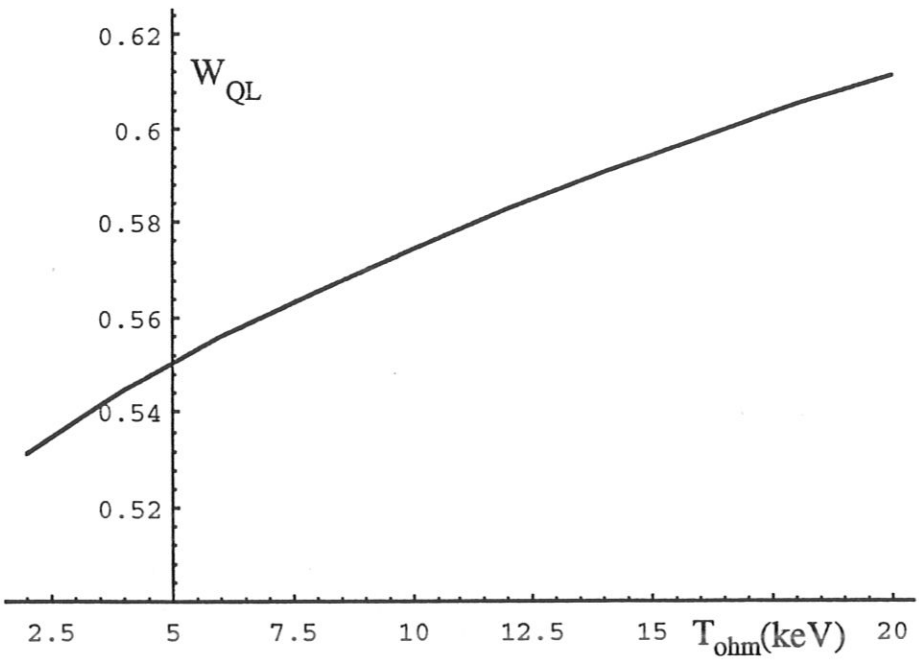


Fig. 19 - ITER first harmonic heating of Deuterium (plasma parameters in Table 1); Quasilinear heating rate vs target plasma temperature for a linear rate of 0.5 W/cm$^3$.

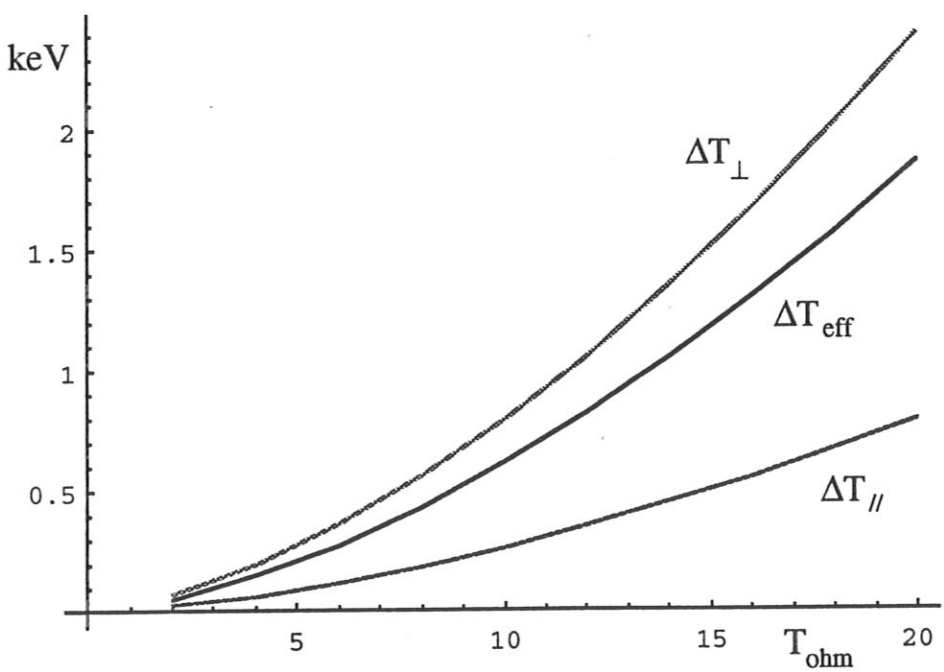


Fig. 20 - ITER first harmonic heating of Duterium (plasma parameters in Table 1); Quasilinear increase of the energy content vs target plasma temperature.

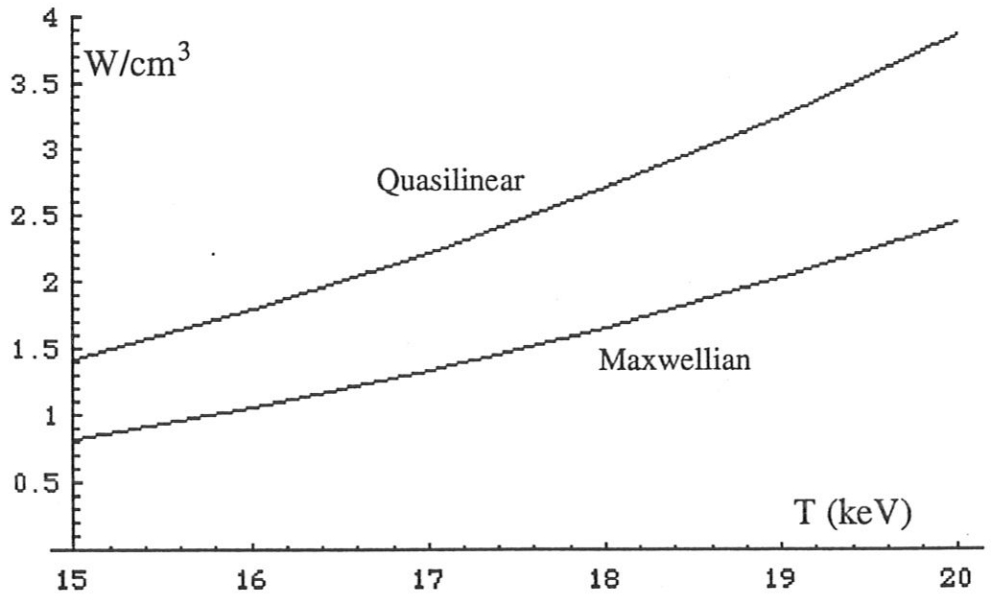


Fig. 21 - ITER first harmonic heating of Tritium (plasma parameters in Table 1); Fusion power vs target plasma temperature for a linear heating rate of 0.5 W/cm$^3$.